

# The role of carbon materials in suppressing dendrite formation in lithium metal batteries

DOU Huang-lin<sup>1,2,3</sup>, ZHAO Zhen-xin<sup>1</sup>, YANG Sun-bin<sup>1</sup>, WANG Xiao-min<sup>1,\*</sup>, YANG Xiao-wei<sup>2,\*</sup>

(1. College of Materials Science and Engineering, Taiyuan University of Technology, Taiyuan 030024, China;

2. School of Chemistry and Chemical Engineering, Shanghai Jiao Tong University, Shanghai 200240, China;

3. School of Environmental Science and Engineering, Taiyuan University of Technology, Jinzhong 030600, China)

**Abstract:** This review highlights several recent models of Li dendrite formation that have been proposed. Based on the comprehensive understanding and insight gained from these models, carbon materials have been developed to prevent the formation of Li dendrites by virtue of their exceptional electrical conductivity, electrochemical stability, mechanical properties and mouldability. A comprehensive review of the advantages of using carbon materials, such as graphene, carbon nanotubes, carbon fibers and hollow carbons, to deal with the formation of Li dendrites in recent years is provided. Finally, the limitations of carbon materials and future research directions for inhibiting Li dendrite formation are summarized as a reference for the development of new carbon materials for high-performance Li metal anodes.

**Key words:** Lithium metal batteries; Lithium dendrite; Carbon materials; SEI; Substrates

## 1 Introduction

As a critical component of energy conversion and storage in transport, power and other industries, secondary batteries continue to push the global industry and energy structure to adjust to the direction of green, environmentally friendly and low-carbon<sup>[1-2]</sup>. The rapid advancement of new energy vehicles has raised the demands for power batteries in terms of energy density, cycle life, and safety performance<sup>[3-4]</sup>. Currently, conventional lithium-ion batteries with graphite anodes are insufficient in meeting the growing demand for electric vehicle range<sup>[5-6]</sup>.

Among all metallic elements known, Li metal stands out as the most ideal electrode material due to its highest theoretical capacity (3 860 mAh g<sup>-1</sup>), lowest electrochemical potential (-3.04 V vs. SHE) and lowest mass density (0.534 g cm<sup>-3</sup> at 20 °C)<sup>[7-8]</sup>. In recent years, research on Li metal batteries (LMBs) with Li metal anodes has become a hot topic both domestically and internationally, making it a key development target for next-generation high energy density batteries<sup>[4,9]</sup>. However, the further commercial implementation of Li metal anodes is impeded by 4 primary

issues: (1) Li dendrite formation, (2) inactive Li accumulation, (3) unstable solid electrolyte interface (SEI), (4) drastic volume change, resulting in shortened lifespan and reduced Coulombic efficiency of LMBs<sup>[4,10-11]</sup>. It should be noted that these challenges are interrelated at various stages of cycling. Amongst these major problems, the uncontrolled formation of high modulus Li dendrites has garnered attention from researchers due to its negative impact on both Coulombic efficiency and safety hazards resulting from the puncturing of the SEI and separator<sup>[12-13]</sup>.

Tremendous efforts have been dedicated to elucidating the mechanism of Li dendrites and Li plating/stripping. The process of Li deposition involves solvated Li ions undergoing mass transfer from the bulk electrolyte to the outer limit of the electrical double layer near the electrode, followed by electro-sorption, desolvation and reduction into adsorbed atoms on the electrode surface<sup>[14]</sup>. The adsorbed atoms diffuse on the surface to reach suitable nucleation sites for Li deposition. The growth of Li dendrites is a complex process that involves various factors, such as Li<sup>+</sup> diffusion and coupling, nucleation and growth,

**Received date:** 2023-05-10; **Revised date:** 2023-06-15

**Corresponding author:** WANG Xiao-min, Ph.D, Professor. E-mail: wangxiaomin@tyut.edu.cn;

YANG Xiao-wei, Ph.D, Professor. E-mail: yangxw@sjtu.edu.cn

**Author introduction:** DOU Huang-lin, Ph.D. E-mail: douhuanglin@tyut.edu.cn

electrolyte properties, SEI characteristics, substrate surface properties and multi-physical field coupling<sup>[15-16]</sup>. To stabilize the Li metal electrode and prevent the formation of Li dendrites, numerous strategies have been developed to regulate the Li deposition behavior. (1) Electrolytes<sup>[17-20]</sup>. The final Li electroplated morphologies are largely determined by the  $\text{Li}^+$  mass transfer in bulk electrolyte. Meanwhile, the solvated structure of  $\text{Li}^+$  in the electrolyte dominates the formation of SEI, which is essential for homogeneous Li deposition<sup>[5]</sup>. Electrolyte additives, super-concentrated electrolytes, and locally highly concentrated electrolyte strategies have been developed to enhance the  $\text{Li}^+$  mass transfer capacity and change the  $\text{Li}^+$  solvation structure<sup>[21-24]</sup>. These improvements aim to promote uniform Li deposition while inhibiting the formation of Li dendrites. (2) SEI<sup>[25-28]</sup>. The highly reactive Li inevitably reacts with the electrolyte components to form a SEI layer. However, due to its insufficient chemical and mechanical stability as well as heterogeneity, the SEI layer can lead to electron tunneling, uneven distribution of  $\text{Li}^+$  flow and interfacial electric field, which exacerbates the formation of Li dendrites<sup>[12]</sup>. For this, the SEI layer was artificially induced to possess uniform composition, stable structure, electronic insulation and ionic conductivity in order to inhibit the growth of Li dendrites<sup>[26]</sup>. (3) Deposition substrates<sup>[29-31]</sup>. Unlike conventional intercalated anodes such as lithium titanate, which have controllable volume expansion, the deposition of Li on metal Li as the substrate or other 2D substrates has virtually infinite volume expansion<sup>[11]</sup>. The large deformation stresses induced by this process are directly associated with the rupture of SEI and the growth of Li dendrites. Tailoring the interfacial energy and lithophilicity between substrates and Li through deposition substrate design provides an effective approach to control Li plating behavior. Meanwhile, following the classical Chazalviel theoretical model, reducing effective local current densities has been validated as an efficacious strategy for mitigating Li dendrite<sup>[32-33]</sup>. Thus, if a suitable 3D substrate can be identified to impede Li metal volume reaction, stabilize SEI and

disperse current density to inhibit Li dendritic growth, the performance of Li metal anodes can be significantly enhanced.

Typically, 3D substrates are constructed predominantly from conducting materials, including metallic materials, carbon-based materials and conducting polymers, to accommodate the rapid conduction of electrons and the reduction of the local current density<sup>[34-35]</sup>. Moreover, 3D conducting substrates can be optimally designed with further modifications to enhance their lithophilicity and homogenize the interfacial  $\text{Li}^+$  distribution, which has very promising applications. The use of 3D metal substrates with high electrical conductivity and mechanical strength is limited by their high cost, relative heaviness, and insufficient chemical and electrochemical stability, which hinders their use in Li metal electrodes<sup>[36-37]</sup>. In comparison, carbon materials with excellent electronic conductivity, light weight, satisfactory mechanical properties, and electrochemical stability have been considered as promising substrates. In addition, carbon-based materials have abundant natural sources and are cost-effective, making them more suitable for commercial applications<sup>[38-39]</sup>. In contrast to traditional metal current collector like copper, they are more inert to HF generated by the decomposition of F-based electrolytes, which are widely used in Li-metal anodes, thereby ensuring substrate structure stability<sup>[37,40]</sup>. Furthermore, carbon-based materials such as graphene, carbon nanotubes and carbon fibers are malleable and can be structurally and functionally designed to meet the requirements of relieving the volumetric effect, rapid mass transfer, uniform electric field, dispersed ion electron flow and rapid nucleation during Li plating/stripping, ultimately inhibiting the growth of Li dendrites and the stability of Li metal electrodes<sup>[32,41-42]</sup>. Consequently, the development of LMBs has been largely facilitated by the adoption of various carbon materials with fruitful successes.

This review primarily focuses on the mechanisms underlying the formation of Li dendrites, including surface diffusion model, heterogeneous nucleation model, space charge model and SEI-induced

nucleating model. Based on classical theoretical models of Li dendrite formation, recent advancements in various advanced carbon materials for stabilizing Li metal anodes, such as graphene, carbon nanotubes, carbon nanofibers and other carbon-based materials, are systematically summarized (Fig. 1). The advantages and limitations of each carbon-based material for suppressing Li dendrites are discussed in detail from structure to chemistry, covering SEI engineering and substrate applications. Finally, a perspective is provided on the current challenges and further rational design of carbon-based materials for Li metal electrodes. The fundamental understanding and technological advances in suppressing Li dendrites by carbon-based materials will facilitate the development of high energy density LMBs.

## 2 Mechanisms of dendrite formation and growth

The uncontrolled growth of Li dendrites poses a significant challenge to the commercialization of LMBs, as they can breach conventional battery separators and cause short circuits, thermal runaway, or even explosions<sup>[43–44]</sup>. In the 1970s, researchers discovered the formation of Li dendrites during charge

and discharge cycles of Li metal anode, and conducted detailed studies on the Li deposition behavior<sup>[45]</sup>. However, the formation mechanism of Li dendrites is a highly intricate process that encompasses various fields such as electrochemistry, crystallography, kinetics and thermodynamics. The origin of Li dendrites remains a topic of debate and there is no universally accepted theoretical models for their growth. Currently, several mainstream models describing the formation of Li dendrites are summarized below.

### 2.1 Surface diffusion model

The surface diffusion process plays a crucial role in the deposition of metals. Desolvated metal ions are reduced to adsorbed atoms by coupling with electrons on the electrode surface, and then diffuse to suitable nucleation sites for nucleation and growth. This process relies on the self-diffusion ability of metal atoms (Fig. 2a)<sup>[46–47]</sup>. From a thermodynamic perspective, the growth of Li dendrites is primarily influenced by lower surface energy and higher migration energy. A decrease in self-diffusion barrier promotes uniform nucleation growth of metal while inhibiting Li dendrite formation<sup>[48–49]</sup>. Through simulation and theoretical analysis, it has been determined that the difference in free energy between low-dimensional and high-dimensional phases of Li is lower compared to other metallic elements such as magnesium. Meanwhile, the self-diffusion on the electrode surface is relatively sluggish, indicating that Li tends to maintain a low-dimensional morphology and preferentially distribute nearby for low-dimensional deposition rather than an ideal two-dimensional planar deposition, which is highly conducive to dendrite growth<sup>[46]</sup>. The model demonstrates that the mobility of interfacial atoms significantly impacts Li dendrite formation. Modifying interface or selecting a deposition substrate to reduce surface self-diffusion barriers and enhance surface migration of Li atoms are effective strategies for guiding uniform Li deposition and inhibiting Li dendrites.

### 2.2 Heterogeneous nucleation model

In most cases, researchers opt for heterogeneous materials as the substrate for Li deposition. During the

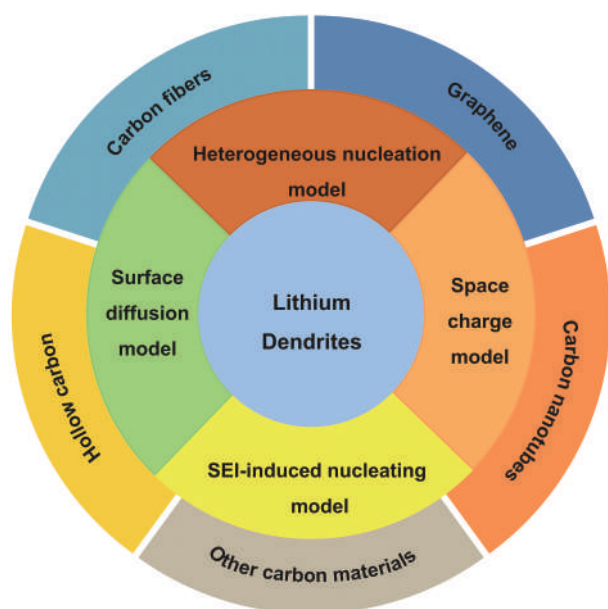


Fig. 1 Schematic summary of Li dendrites formation models and advanced carbon materials

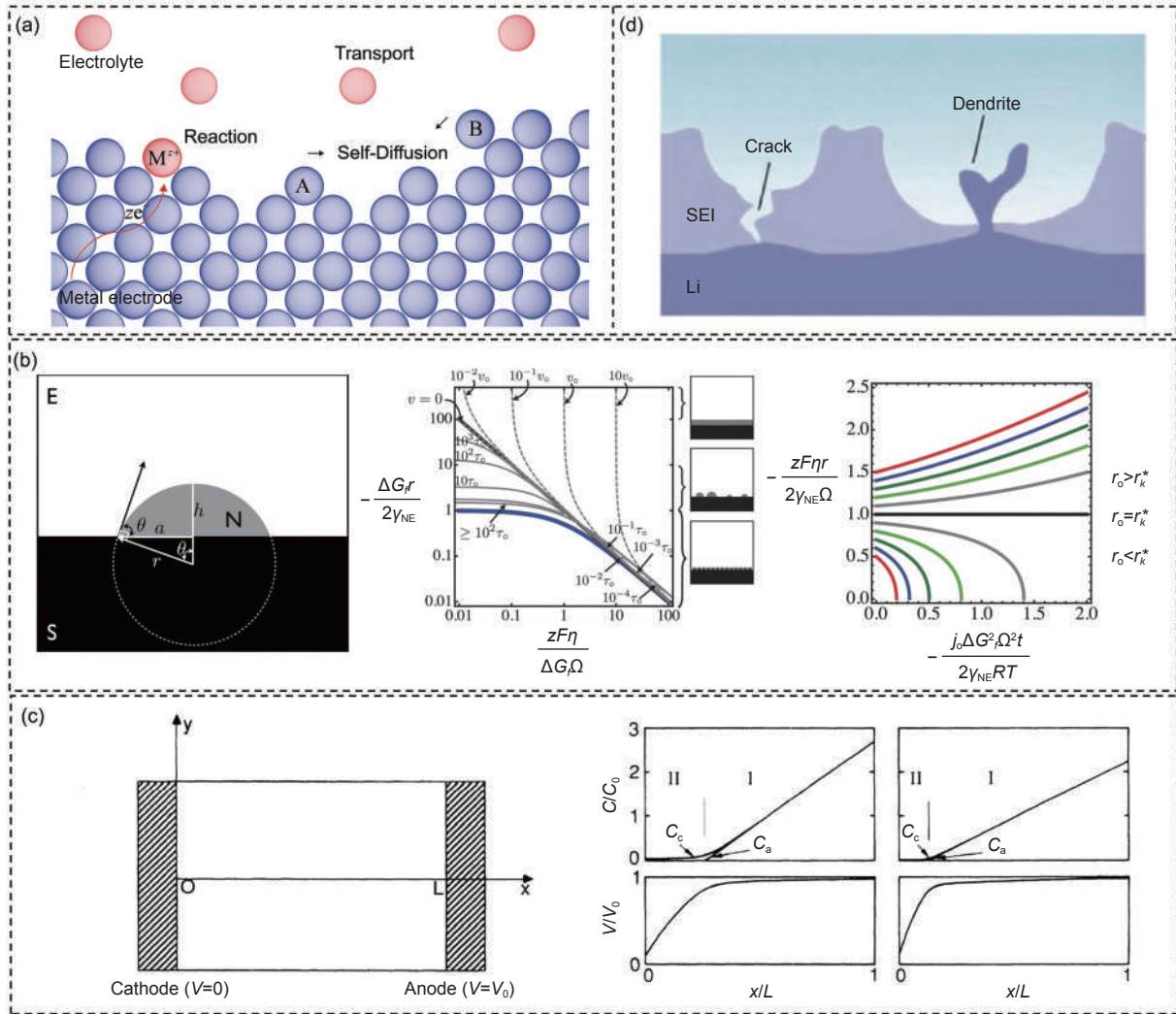


Fig. 2 (a) Schematic illustration of electrodeposition<sup>[47]</sup>. (b) Schematic illustration of a nucleus with a spherical cap shape. Behavioral patterns during the early stages of nucleation and growth, and the growth electrodeposit size varies with time<sup>[50]</sup>. (c) Scheme of the cell. The relationship between ion concentration  $C_c$  and  $C_a$ , and the electrostatic potential<sup>[51]</sup>. (d) A nonuniform SEI renders irregular Li deposition<sup>[56]</sup>. (Reprinted with permission)

initial stage,  $\text{Li}^+$  acquire electrons and deposit on the current collector through a process of heterogeneous nucleation that determines both the uniformity of initial deposition and subsequent morphology of Li deposition, including Li dendrite formation. Therefore, a comprehensive understanding of heterogeneous nucleation is imperative. Ely and Garcia proposed a heterogeneous nucleation model based on theoretical simulation to establish a correlation between the initial stages of heterogeneous nucleation and the formation of Li dendrites<sup>[11,50]</sup>. The process of Li's heterogeneous nucleation involves 4 distinct steps: (1) Nucleation suppression. At this stage, the thermodynamically unstable embryos cannot be effectively separated from the electrolyte. (2) Long-term incubation. In this

process, the thermodynamics of the system gradually tends to stabilize, allowing for retention and gradual growth of the incubated embryos. (3) Short-term incubation. Driven by the overpotential, the embryo undergoes rapid growth until it reaches its critical kinetic size, at which point it is primed for the formation of a Li nucleus that is both thermodynamically and dynamically stable. (4) Growth stage. This stage can be divided into 2 phases: early growth and late growth. During this process, the embryo undergoes thermodynamic and kinetic stabilization before reaching its final nucleus size. Once the Li nucleus reaches a stable state of development, its growth rate will remain constant until it achieves its desired form. According to this model, the formation of Li embryos requires

reaching a critical thermodynamic radius, while maintaining their growth necessitates achieving a critical kinetic radius (Fig. 2b)<sup>[11,50]</sup>. The growth of Li dendrites can be effectively controlled or regulated by adjusting the Li nucleation process, ensuring that the particle size of the anode is smaller than the critical thermodynamic radius and optimizing substrate surface smoothness and lithophilicity.

### 2.3 Space charge model

This model is widely employed in the investigation of Li dendrite growth and inhibition, enabling the quantification of Li dendrite formation<sup>[12]</sup>. Chazalviel et al. postulated that cation migration in dilute electrolytic liquid systems is primarily driven by diffusion<sup>[33,51]</sup>. However, if  $\text{Li}^+$  are deposited rapidly on the electrode surface and the near-surface  $\text{Li}^+$  are consumed quickly without being replenished, a depletion zone will form, generating a localized space charge layer and establishing an electric field. Subsequently, the  $\text{Li}^+$  migration in this region is governed by an electric field with a significantly lower potential than that of the anode (Region II). The intense electric field electroadsorbs and electroplates numerous cations within a short time frame, leading to non-uniform Li deposition behavior and ultimately resulting in the formation of Li dendrites (Fig. 2c). This model adheres to the Sand's law proposed by Henry J S Sand, which states that dendrite generation occurs when the  $\text{Li}^+$  concentration on the electrode surface reaches 0, also known as Sand's time<sup>[52-53]</sup>. The space charge model is widely accepted due to its establishment of the relationship between Sand's time and diffusion constant, provision of a quantitative calculation method for dendrite formation time, and correlation of the relationship between applied current density and dendrite formation. This theoretical model provides a large number of effective ideas for inhibiting the formation of Li dendrites, including improving the cationic conductivity/migration number or fixing anions to relieve space charge, using three-dimensional conductive substrates to reduce local current density, etc., and has been demonstrated by extensive research results.

### 2.4 SEI-induced nucleating model

Due to the high reactivity of Li, it readily reacts with electrolyte components to form a SEI layer between the solid and liquid phases<sup>[54]</sup>. This also implies that during deposition,  $\text{Li}^+$  must undergo a process of solid-state migration within the SEI, which can significantly impact the final morphology of Li deposition<sup>[55]</sup>. However, the SEI interface chemistry has not been thoroughly examined in the theoretical models of Li dendrite formation summarized above. Under ideal conditions,  $\text{Li}^+$  permeate through the SEI layer and deposit beneath it, thereby challenging the mechanical properties of SEI due to volume expansion caused by Li deposition<sup>[27]</sup>. Once the SEI fractures under stress, an electrochemical hot spot is generated, leading to preferential deposition of  $\text{Li}^+$  inhomogeneously and dendritically within the bare Li region lacking SEI coverage. Simultaneously, the exposed Li will undergo continuous side reactions with the electrolyte, resulting in ongoing consumption of both electrolyte and active Li (Fig. 2d)<sup>[12,56]</sup>. This leads to an accumulation of inactive Li which further contributes to the formation of dendrites until they penetrate the separator and cause a short circuit. On the other hand, the formation of Li dendrites is directly influenced by both the composition distribution of SEI layer and the diffusion rate of  $\text{Li}^+$ . The inhomogeneity in composition and structure of SEI can result in uneven distribution of  $\text{Li}^+$  flow, thereby promoting generation of Li dendrites. The resistance to  $\text{Li}^+$  diffusion in the SEI reflects the overpotential during deposition and significantly impacts the morphology of deposits. Based on this theoretical model, researchers have optimized the design of artificial SEI by preconstructing or electrolytic chemistry to construct LiF-rich SEI layers. These improvements enhance the SEI modulus and  $\text{Li}^+$  transport capacity, effectively inhibiting the formation of Li dendrites<sup>[24,57-59]</sup>. Furthermore, significant efforts have been made in constructing SEI through introducing alloy components and polymer components, successfully demonstrating its effectiveness in suppressing dendrite growth<sup>[60-63]</sup>.

In general, the above theoretical models describe

the formation of Li dendrites from the perspectives of self-diffusion, nucleation, interface, thermodynamics and dynamics<sup>[12]</sup>. However, as the Li dendrite problem is being studied in greater depth, it has become apparent that the aforementioned theoretical models of Li dendrite formation are insufficient to fully describe the complex process of Li dendrite growth. Meanwhile, ongoing research is constantly enriching our understanding of the formation of Li dendrites by identifying new factors that affect it, including mechanical, electrical and other physical field factors. These theoretical models provide researchers with multiple perspectives on Li dendrites and offer a range of ideas and methods to address the issue.

### 3 Carbon materials for suppressing Li dendrites growth

In lithium-ion batteries, in addition to being the active electrode material for the anode, carbon materials play an important role as a carrier structure for other active materials due to their strong plasticity, and as a conductive agent for both electrodes<sup>[64-65]</sup>. To provide increased gravimetric energy density, carbon materials, thanks to features like light weight, high conductivity, malleability, chemical and electrochemical stability and high mechanical strength, also play an important part in constructing stable Li metal anodes<sup>[66-67]</sup>. Although the theory of Li dendrite formation is not yet perfect, optimizing Li plating/stripping from the perspective of nucleation, SEI and substrate design based on several models mentioned above can be effective<sup>[68-70]</sup>. Advanced carbon materials, such as graphene, carbon nanotubes, carbon fibers and hollow carbon have shown great potential in guiding Li plating/stripping and suppressing Li dendrites. They are particularly effective in building artificial SEI layers and depositing substrates.

#### 3.1 Graphene

Graphene is a 2D monolayer carbon material with  $sp^2$  hybridization, exhibiting excellent electron conductivity ( $\sim 2\,000\text{ S cm}^{-1}$ ) and specific surface area (SSA) ( $\sim 1\,500\text{ m}^2\text{ g}^{-1}$ )<sup>[42,64]</sup>. Additionally, both graphene and reduced graphene oxide (rGO) possess

remarkable structural stability and plasticity<sup>[37]</sup>. Owing to these advantages, graphene materials have been extensively employed in the construction of high-performance Li metal electrodes in recent years, including artificial SEI layers as well as 2D or 3D substrates for Li deposition<sup>[38,71]</sup>.

Recent studies have reported that graphene, thanks to its high mechanical strength, can effectively inhibit the formation of Li dendrites by regulating the SEI layer. Wei et al. utilized a spraying method to coat the Li metal surface with graphene oxide (GO), which was then spontaneously reduced due to the strong reducibility of Li, resulting in the formation of SEI on its surface (Fig. 3a)<sup>[72]</sup>. The symmetric cell assembled can maintain stability for 1 000 cycles with negligible overpotential increase at  $5\text{ mA cm}^{-2}$ . Therefore, the SEI layer formed by graphene's high mechanical strength can effectively inhibit the formation of Li dendrites, as confirmed by other work<sup>[73]</sup>. Based on graphene, the incorporation of other components to enhance SEI-Li affinity and regulate nucleation barriers can more effectively inhibit Li dendrites. Cheng et al. have reported an artificial interface of GO-BQ@LiTFSI (GBL) with abundant lithiophilic active site groups, which can assist the formation of a LiF-rich SEI. The synergistic effect between GBL and SEI not only effectively suppresses Li dendrite formation due to the intrinsic high modulus of GO, but also regulates  $\text{Li}^+$  flux distribution<sup>[74]</sup>. After incorporating the GBL into symmetric cells, an excellent cycling performance was obtained ( $600\text{ h}$  at  $3\text{ mA cm}^{-2}$  with  $3\text{ mAh cm}^{-2}$ ) (Fig. 3b). Although some researchers have reported the use of graphene as SEI layer to enhance Li deposition behavior, its suitability for this purpose is limited due to the high electronic insulation requirements of SEI. Generally, in order to better exhibit the mechanical properties and other characteristics of graphene and inhibit the formation of Li dendrites, it is necessary to combine graphene with other insulating components or functionalize it to construct a new insulated interface.

In fact, graphene is more suitable as Li deposition substrate than as SEI layer. In 2016, Zhang et al.

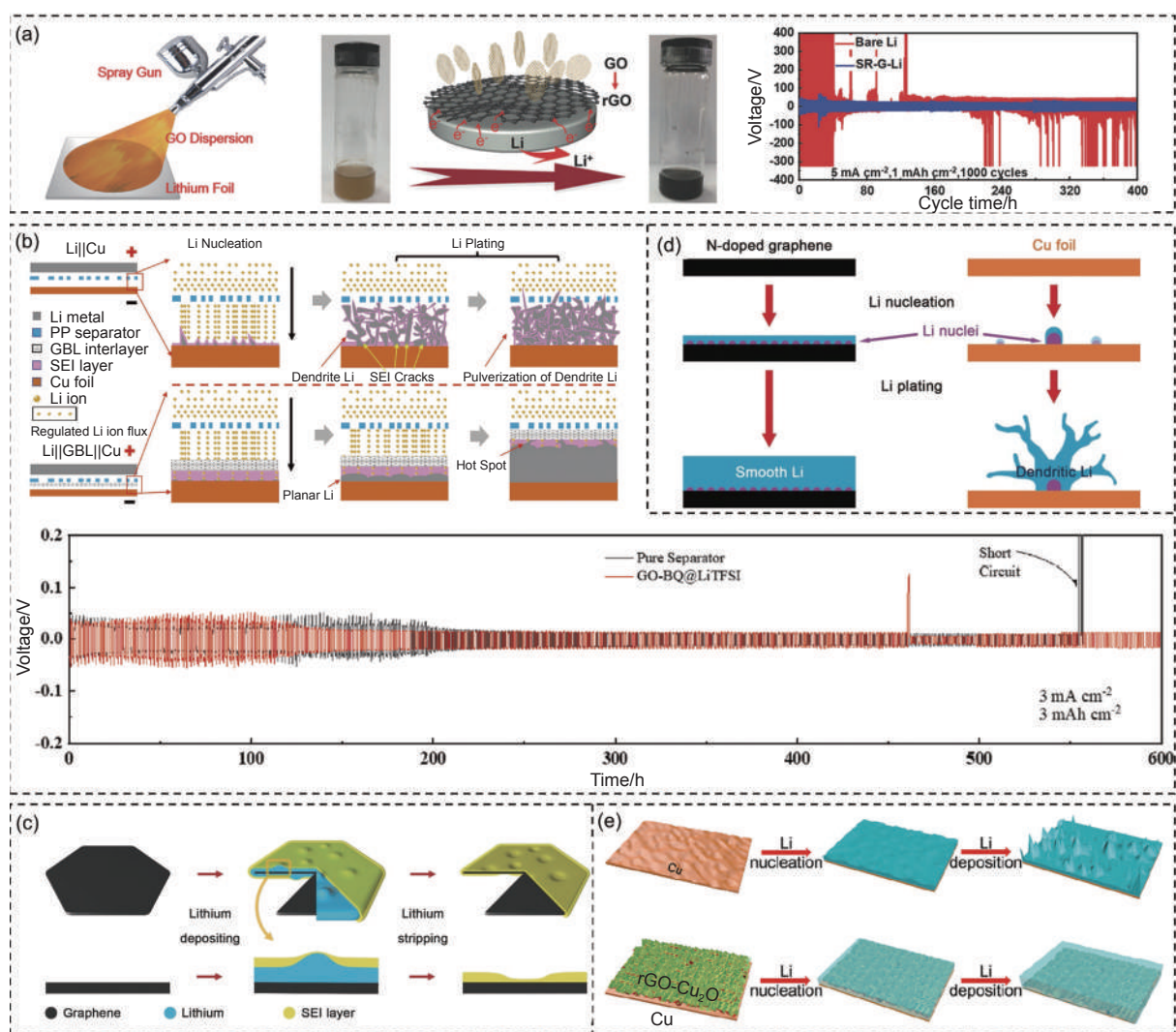


Fig. 3 (a) Schematic diagram of the spray process and optical image of the reduction process for the preparation of SR-G-Li. The cycling stability of the bare Li and SR-G-Li electrodes at 5 mA cm<sup>-2</sup>[72]. (b) Schematic illustration of Li deposition on Cu and GBL||Cu. The cycling performance at 3.0 mA cm<sup>-2</sup> with 3 mAh cm<sup>-2</sup>[74]. (c) Schematic illustration of Li depositing and stripping on graphene substrate[75]. (d) Comparative diagram of Li nucleation and plating on N-doped graphene and copper foil[77]. (e) Schematic diagram of Li nucleation and deposition on the Cu foil and rGO-Cu<sub>2</sub>O/Cu[80]. (Reprinted with permission)

proposed the concept of utilizing non-stacked graphene with high SSA, pore volume and electrical conductivity as a substrate to guide Li deposition for reducing local current density and inhibiting dendrite formation in graphene-Li metal composite electrodes (Fig. 3c)[75]. Additionally, a sandwich-like structure with graphene at its core, Li in the outer layer, and SEI in the outermost layer was fabricated by combining the SEI layer induced by LiTFSI-LiFSI double salt ether base electrolyte. This structure has been proven to increase Coulombic efficiency of LMBs. However, it should be noted that the Li nucleation on the basal plane of single-layer graphene is much more challenging than that on Cu under the same current density or

Li deposition capacity. As the amount of deposited Li increases, dendrites are more likely to form from Li nuclei. Therefore, lithiophilic defects and functional groups need to be introduced onto the basal plane of graphene[76]. In view of this, Zhang et al. used heteroatomic doping to enhance the lithiophilicity of graphene and serve as the Li deposition substrate (Fig. 3d)[77]. When nitrogen(N) is doped onto graphene, lithiophilic functional groups such as pyridinic and pyrrolic nitrogen provide a smaller nucleation barrier and more uniform distribution of nucleation points compared to copper substrate, inhibiting Li dendrite growth and exhibiting a high Coulombic efficiency of 98% for nearly 200 cycles. It should be

noted that excessive N content may destroy the conjugated structure of graphene and reduce conductivity, making them unsuitable for Li deposition. This doping concept is further expanded by introducing S, F and other elements to enhance the lipophilicity of graphene, exhibiting excellent performance in inhibiting Li dendrite growth<sup>[78-79]</sup>. In addition to heteroatomic doping, combining other components is also an effective method for enhancing the lipophilicity of graphene and inducing uniform Li deposition. Wang et al. proposed a rGO and Cu<sub>2</sub>O co-modified Cu substrate, which lower the nucleation barrier, induce Li nucleation, and promote charge transfer due to the conductive rGO generated, resulting in a uniform electric field distribution and inhibition of Li dendrite formation (Fig. 3e)<sup>[80]</sup>.

Under the guidance of Sand's Law, the construction of a 3D Li deposition substrate can effectively homogenize ion flux and reduce local current density, thereby regulating Li deposition and inhibiting the growth of Li dendrites. Due to its excellent plasticity, graphene exhibits promising prospects in constructing a 3D Li deposition substrate. Cui et al. reported a composite Li metal anode with 7% (mass fraction) 'lithiophilic' layered rGO as the Li substrate<sup>[81]</sup>. The spark reaction initiates the injection of molten Li into a rGO film with uniform nanogaps, resulting in a uniformly periodic stacking of nano-scale Li and rGO (Fig. 4a). This process significantly mitigates the volume effect of Li (approximately 20%-dimension variation) during cycling, ensuring uniform Li deposition and stripping. Meanwhile, the top layer of rGO can serve as an artificial SEI to enhance the stability of composite metal electrodes. In subsequent research, Cui et al. incorporated silicon nanoparticles into this substrate constructed by nucleation points to further optimize Li deposition behavior<sup>[82]</sup>. A similar approach was further developed by Cao and Wu to construct a conductive and lithophilic 3D MXene/graphene framework for dendrite-free Li metal anodes<sup>[83-84]</sup>. However, as previously mentioned, the untreated pure graphene exhibits insufficient affinity for Li, which hinders the Li nucleation on its surface. Therefore, a

strategy involving tailored carbon nanoparticles with specific shape and electronic properties can be employed to facilitate zero overpotential Li nucleation on sp<sup>2</sup> carbon substrates<sup>[85]</sup>. As shown in Fig. 4b, Wei et al. reported a 3D carbon nanofiber (CNF) substrate of vertically grown edge-rich graphene which not only exhibits excellent electronic properties and open structure but can also act as a nanosite to achieve 0 nucleation overpotential and guide Li to uniformly deposit without dendrites<sup>[86]</sup>. Further advancements have been made in the development of similar strategies for constructing 3D substrates in collaboration with other components, such as graphene and g-C<sub>3</sub>N<sub>4</sub>, to effectively remove Li dendrites<sup>[87]</sup>. Xu et al. fabricated a tent-shaped artificial interface (TLI-GO/Zn/CC) via the self-assembly of GO on Zn nanosheets (Fig. 4c), which effectively confines the spatial distribution of Li plating and ultimately obtains a stable composite Li metal anode<sup>[7]</sup>. A tented interface with a nano-cavity is constructed, wherein the nano-cavity provides space for the Li deposition/stripping. The Li metal is confined inside the nano-cavity to effectively reduce direct contact between electrolyte and Li metal, minimize side reactions, and decrease continuous consumption of electrolyte and Li metal. The self-assembly of GO results in the formation of Zn-O-C covalent bonds, which serve as anchor points for attaching the GO layer to the substrate material and ensure its stability during cycling. Additionally, due to its lithophilic properties, the Zn-O-C bond can facilitate Li deposition within nanocavities. The tented interface significantly enhances the electrochemical performance of TLI-GO/Zn/CC anode. The symmetric battery exhibits stable cycling for 1 600 h at a current density of 1 mAh cm<sup>-2</sup>, and the full cell retains 94.6% capacity after 3 000 cycles at a high rate of 5 C.

In general, although pure 2D graphene exhibits excellent film-forming properties, its exceptional conductivity cannot prevent the occurrence of side reactions without modification, rendering it unsuitable as a stable SEI layer. In contrast, graphene with high plasticity is more suitable as a 3D substrate for guiding the uniform Li deposition.

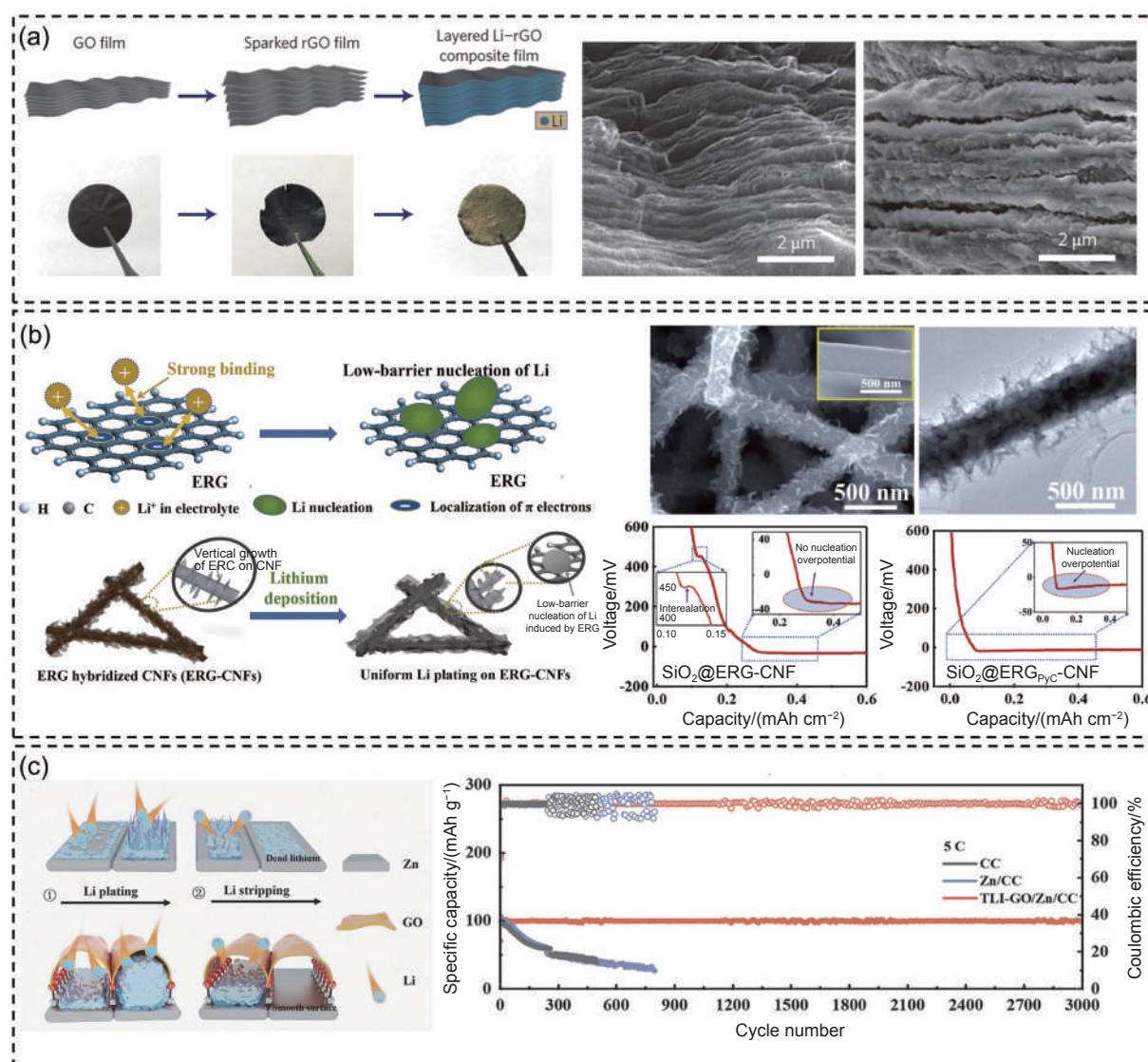


Fig. 4 (a) Schematic diagram of preparation of the sparked rGO films and layered Li-rGO composite film, and the corresponding SEM images<sup>[81]</sup>. (b) Schematic diagram of the 0 V overpotential Li nucleation on ERG and uniform Li plating on the ERG-hybridized 3D CNF substrate. Deposition curves of Li at 0.2 mA cm<sup>-2</sup> on SiO<sub>2</sub>@ERG-CNF and SiO<sub>2</sub>@ERGP<sub>PyC</sub>-CNF<sup>[86]</sup>. (c) Schematic illustration of Li plating and stripping on bare Zn and the Zn with tent-like nanocavities interface anchored by Zn-O-C bond. The cycling stability of Li||LFP cells with different Li anodes at 5 C<sup>[7]</sup>. (Reprinted with permission)

However, the low affinity of pure graphene towards Li makes it unsuitable for rapid nucleation and growth. The incorporation of functional groups, heteroatomic doping, and recombination of lithiophilic components can effectively lower the nucleation barrier for Li deposition and achieve a stable morphology during plating/stripping cycles, which is conducive to dendrite suppression and improvement in electrochemical performance. In addition, as a host material, careful attention must be paid to the design of graphene's pore structure and stacking mode due to its unfavorable effect on spatial transport.

### 3.2 Carbon nanotubes

Compared to 2D graphene, carbon nanotubes (CNTs) are one-dimensional (1D) nanomaterials composed of sp<sup>2</sup> hybrid carbon atoms. They possess a light weight and a perfectly connected hexagonal structure, exhibiting outstanding mechanical, electrical and chemical properties. The unique 1D structure of CNTs endows them with strong plasticity and composability. For the Li metal electrode, it can be manipulated to form a Li deposition substrate or composite with other components to construct a substrate together. This results in rapid electron transmission and dis-

persed current density abilities, making it highly promising for Li dendrite suppression.

As previously mentioned, the 1D morphology and properties of CNTs make them more suitable for constructing 3D host structures for Li. Wu et al. have successfully prepared a dendrite-free Li/CNTs hybrid material for LMBs by directly coating molten Li onto CNTs (Fig. 5a). The reasonable supercooling conditions applied to the molten Li result in pressures far exceeding its gravitational differential pressure<sup>[88]</sup>. The Li core is elevated, allowing for the infusion of molten Li into a CNT sponge film (CSMF), obtaining a homogeneous mixture of molten Li coated CSMF (LiCSMF) which possessed ample active sites and balanced electric fields distribution, facilitating Li<sup>+</sup> transport during charge and discharge. The prepared LiCSMF electrode can cycle 2 000 times even at 40 mA cm<sup>-2</sup>, showing a superstable cycling performance. CNT is used to construct composite Li metal anode, which not only disperses current density, but also provides conductive path for “dead Li” to a certain extent, so as to realize efficient utilization of Li metal<sup>[89]</sup>. The incorporation of additional lithiophilic components into the Li deposition substrates constructed by CNTs can further enhance the affinity between the CNTs substrates and Li, thereby inhibiting the formation of Li dendrites<sup>[90]</sup>. By implementing a zinc oxide (ZnO) load gradient reduction, Mai et al. were able to achieve a lithiophilic and lipophobic interface layer<sup>[91]</sup>. The bottom layer of CNTs coated with ZnO exhibited lithiophilic properties that facilitated the uniform formation of the SEI layer while inhibiting the growth of Li dendrites (Fig. 5b). Meanwhile, the top layer is lithiophobic CNT with high mechanical strength and porous structure, which effectively suppressed Li dendrite growth and promoted Li<sup>+</sup> diffusion. In combination with the high plasticity of CNT and the lithophilicity of ZnO, various approaches have been employed to integrate them for constructing Li metal electrodes that can effectively suppress the formation of dendrites<sup>[92]</sup>.

Chen et al. reported a kind of Li-CNT-acetylene

black (Li-CNT-AB) composite microsphere electrode material<sup>[93]</sup>. Lithiophilic carbon nanotubes (CNTs) were employed to fabricate a porous spherical framework, within which lithiophilic AB particles were distributed to exploit the pore space of the spheres (Fig. 5c). This strategy effectively enhanced the Li content of composites and served as an accelerator for Li deposition during battery cycling due to their low nucleation barrier and excellent inhibition properties against dendrite growth. Later, Chen et al. pioneered the application of single molecular layer self-assembly (SAM) in surface protection of Li metal<sup>[94]</sup>. Octadecylphosphinic acid (OPA) molecules were utilized to coat Li-CNT composites, and SFG characterization revealed that OPA assembled on Li-CNT in a single molecular layer mode (Fig. 5d). The alkyl chains of OPA exhibit excellent water repellency, while the monolayer coating is too thin to impede Li<sup>+</sup> and electrons. The coated Li metal exhibits excellent stability in dry air and is highly compatible with specific solvents, enabling the preparation of a Li metal cathode through mixed slurry coating. Additionally, the monomolecular layer provides protection for the Li metal during electrochemical cycling.

In brief, the application of 1D CNTs in SEI has not been widely explored, but they exhibit promising potential as a 3D Li deposition substrate. While maintaining the excellent electrical conductivity of carbon materials, the high plasticity and compatibility of CNTs facilitate their combination with other active materials and enable precise structural design. This shows great potential in inhibiting the formation of Li dendrites by reducing the Li nucleation barrier, directing the Li<sup>+</sup> flow distribution, and reducing the local current density. However, achieving a balance between pore structure, density of CNTs, electrochemically inert components (such as lithiophilic materials), and battery performance is critical and worthy of consideration for further applications.

### 3.3 Carbon fibers

Carbon fiber (CF) is an optimal material for constructing high-performance composite Li metal anodes because of its exceptional SSA, excellent elec-

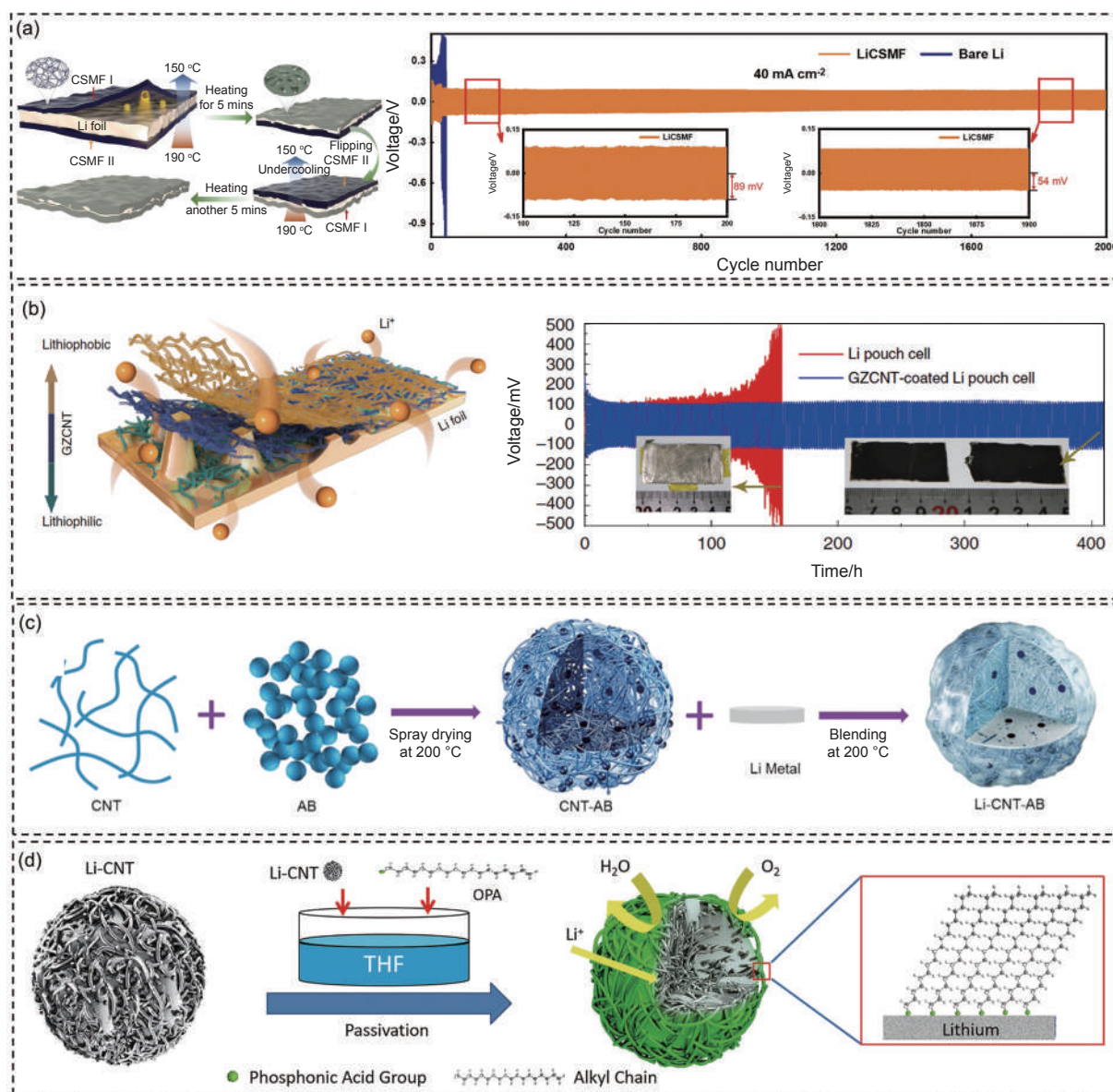


Fig. 5 (a) Schematic diagram of preparation of the LiCSMF electrode. Cycling performance at 40 mA cm<sup>-2</sup> with 2 mAh cm<sup>-2</sup>[88]. (b) Schematic illustration of Li deposition on Li foils with GZCNT interface, and the cycling stability of the pouch cells of Li foils with/without GZCNT at 1 mA cm<sup>-2</sup> with 1 mAh cm<sup>-2</sup>[91]. (c) Schematic of preparation of the Li-CNT-AB[93]. (d) Schematic diagram of the preparation of OPA-Li-CNT sphere by molecular self-assembly[94]. (Reprinted with permission)

tron conductivity, low density and remarkable electrochemical stability<sup>[95]</sup>. To tackle the issue of uneven Li deposition at high current density and achieve high areal capacity, the development of heterogeneous seed decorated 3D substrate is an effective strategy to impede the proliferation of Li dendrites. However, the mechanical and electrochemical stability of these nano seeds are pivotal prerequisites for ensuring prolonged cycling performance of LMBs and need to be taken seriously.

It should be noted that, in the micrometer-scale

CF substrates, the capacity provided by the intercalation reaction cannot be disregarded alongside the deposited Li. Guo et al. designed a self-supporting 3D multifunctional graphitized carbon fiber as a collector for Li metal anode (Fig. 6a)<sup>[96]</sup>. Using a commercial freestanding graphitized carbon fiber (GCF) electrode as a 3D substrate offers several advantages: (1) The GCF electrode facilitates Li intercalation and deposition, resulting in a remarkable enhancement in Li storage capacity, and ultra-high areal capacity of 8 mAh cm<sup>-2</sup> can be gained using this multifunctional 3D

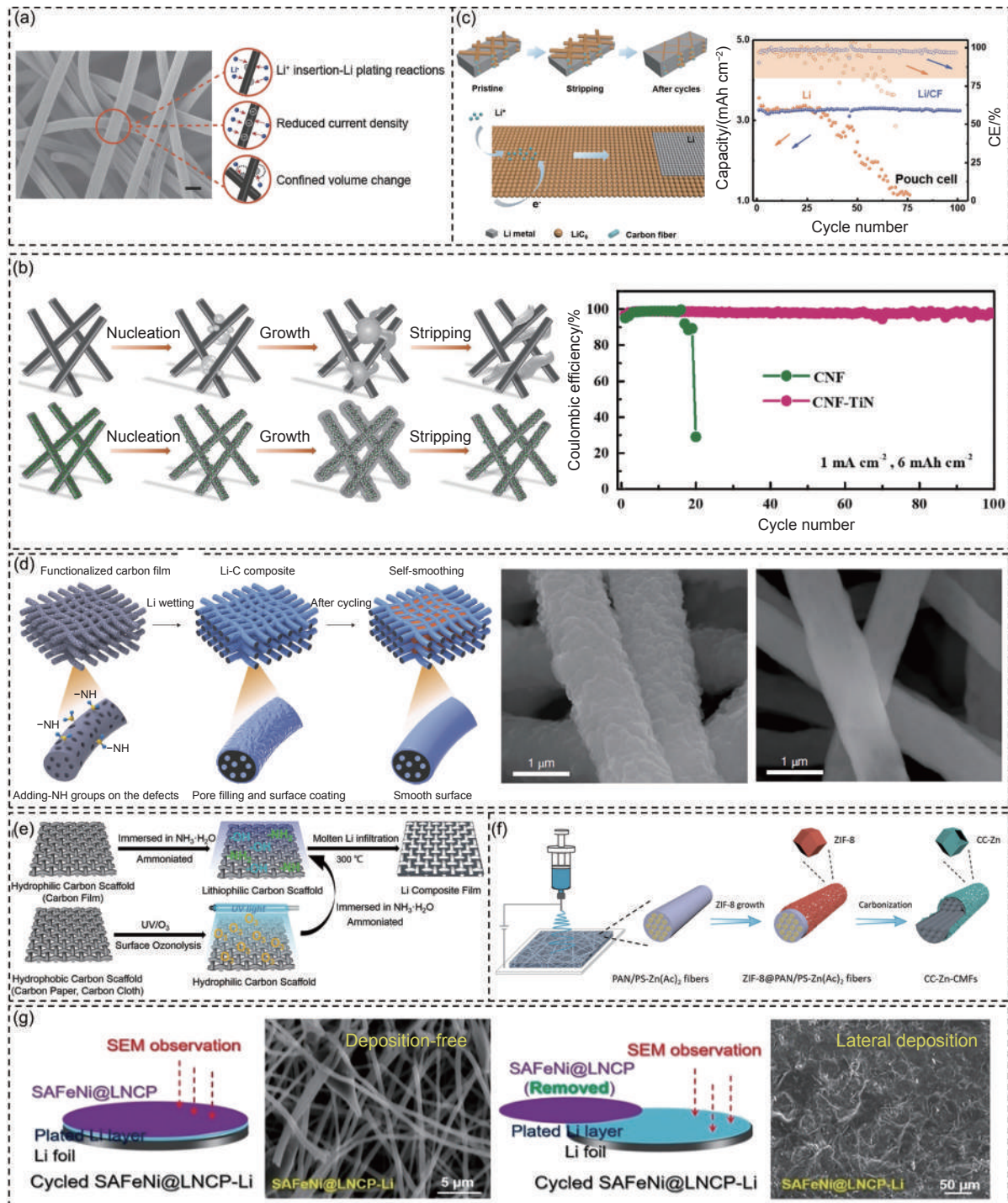


Fig. 6 (a) SEM image and the multifunctionality of GCF electrode<sup>[96]</sup>. (b) Schematic illustration of Li deposition and stripping on the CNF and CNF-TiN, and the corresponding CE profiles at  $1 \text{ mA cm}^{-2}$  with  $6 \text{ mAh cm}^{-2}$ <sup>[98]</sup>. (c) Schematic diagram of Li plating/stripping behavior on Li/CF composite anode, and the performance of pouch cells with S cathodes<sup>[99]</sup>. (d) Schematic representation of the self-smoothness of the Li-C electrode in cycling. SEM images of the pristine and cycled Li-C electrode<sup>[100]</sup>. (e) Schematic of the Li composite film prepared with hydrophilic or hydrophobic carbon scaffolds<sup>[101]</sup>. (f) Schematic diagram of the preparation of CC-Zn-CMFs<sup>[102]</sup>. (g) Schematic and SEM image of the cycled electrode with/without upper SAFeNi@LNCP modulation layer<sup>[103]</sup>. (Reprinted with permission)

collector. (2) The large SSA provided by CF reduces local current density and promotes homogeneous Li plating. (3) The porous structure of the 3D collector

can effectively mitigate the volume changes during cycling<sup>[97]</sup>. However, an excessively high intercalation capacity may compromise the energy density of

Li metal anodes; thus, it is necessary to balance the intercalation and deposition capacity.

To further restrict the formation of Li dendrites, CF materials decorated with heterogeneous seeds or surface functionalization of CF materials can optimize the Li deposition on these substrates while impeding the proliferation of Li dendrites. Li et al. developed a TiN nanoparticle-modified 3D carbon nanofiber (CNF) mat that can be used as Li deposition substrate (Fig. 6b)<sup>[98]</sup>. The homogeneous Li plating was obtained by the synergistic effect of TiN and the 3D CNF structure with excellent conductive framework. Li was preferentially adsorbed on lithiophilic TiN due to its low diffusion energy barriers. Moreover, the pseudocapacitive property of TiN as determined by kinetic characteristic facilitated high-rated Li<sup>+</sup> storage and charge transfer processes. The electrochemical performance of the Li metal anode based on CNF-TiN is significantly enhanced, enabling stable operation for 200 cycles at 3 mA cm<sup>-2</sup>, as well as a long cycling life. Zhang et al. have developed a facile and scalable method, operable at room-temperature for preparing lithium-carbon composite anodes by rolling an ultra-thin layer of Li metal onto CFs to form a prelithiation coating through the spontaneous generation of LiC<sub>6</sub> via the reaction between Li and graphite (Fig. 6c)<sup>[99]</sup>. The electronegativity of carbon atoms is enhanced, thereby strengthening the bond between the carbon skeleton and Li<sup>+</sup>, effectively mitigating volume change, dendrite growth and pulverization caused by Li deposition. The S||Li/CF pouch cell displays a high capacity of 3.25 mAh cm<sup>-2</sup> and maintain 98% capacity after 100 cycles.

Liu et al. used amine-functionalized 3D mesoporous CFs to provide stable Li-C anodes for high energy density LMBS<sup>[100]</sup>. The preferential Li nucleation and growth in pores and cavities under the action of amine on carbon substrate enables uniform Li deposition during operation (Fig. 6d). The gradual smoothing of the rough electrode surface observed in the early-stage contrasts with the conventional formation of large Li dendrites on flat Li metal. When com-

bined with a high-capacity cathode, this thin Li-C anode enables a full cell with an energy density of 350-380 Wh kg<sup>-1</sup> and cycling stability (over 200 cycles). Reasonable treatment of functional groups on CF can effectively enhance the lithiophilicity of CF, promoting the Li adsorption and nucleation. Furthermore, it can optimize the electrolyte-electrode contact, which is highly beneficial for guiding uniform Li plating and efficiently inhibiting dendrite growth. Lin et al. reported a lignin-derived CF membrane modified by mild surface ozonolysis and ammoniation (Fig. 6e), which effectively improved the permeability of Li in the carbon matrices, making it easier for molten metallic Li to infiltrate into this carbon substrates<sup>[101]</sup>. The authors prepared a Li@carbon fibre film (Li@CF) composite metal electrode with 3 222 mAh g<sup>-1</sup>. After deep charge/discharge pre-cycling, a uniform, thick Li was formed in the Li@CF electrode, effectively suppressing volume expansion and dendrite formation.

Lou et al. constructed a 3D host composed of N-doped amorphous Zn-C multichannel fibers (CC-Zn-CMFs) that were modified with carbon cages (CCs)<sup>[102]</sup>. The 3D conductive layered CFs possess a large SSA, which can effectively facilitate electron transport and reduce local current density (Fig. 6f). The multi-channel carbon fibers with nanocages in their large pore structures are capable of accommodating significant volume changes during long electrochemical cycling. Moreover, the N-doped carbon and Zn nanoparticles exhibit an enhanced anchoring effect on Li<sup>+</sup> due to their ultra-low superpotential. This effectively controls Li nucleation and growth, allowing for directional deposition onto the layered carbon. Lin et al. employed density functional theory (DFT) simulations to investigate the potential of single-atom catalyst activators in modulating the diffusion kinetics and Li plating behavior (Fig. 6g)<sup>[103]</sup>. Simulations were conducted to determine the surface diffusion energy barriers involved in the formation and breaking of Li dimers between neighboring Li atoms (away from other Li atoms) on various substrates, with a focus on modeling the electrochemical diffusion process. The results indicate that atomic iron and nickel

catalysts, well-distributed throughout ultralight N-doped carbon nanofiber paper (SAFeNi@LNCP), significantly enhance both Li surface diffusion and lateral distribution. The mobility of neutral Li is non-negligible, and the atomic surface diffusion rate is significantly promoted by single-atom catalysts. A series of characteristics reveal that SACs act as kinetic activators to promote the Li surface diffusion and lateral redistribution, thereby achieving uniform Li deposition.

As another 1D carbon material, CF offers a more cost-effective advantage compared to CNTs. Its diameter can range from nano to microscopic, and its structure can be transformed from solid to hollow, providing an optimal pathway for Li storage. Therefore, it is widely utilized in related research on Li metal electrodes. However, further functionalization or combination with other active ingredients is necessary to reduce the Li nucleation barrier and inhibit the formation of dendritic Li. Additionally, during the further functionalization of CF, its mechanical strength may be significantly reduced, which is also a crucial consideration for Li metal substrates.

### 3.4 Hollow carbon

Compared to other carbon materials, hollow carbon materials with unique hollow configurations exhibit superior mechanical strength, electrical conductivity, low density and abundant micro-mesoporous distribution. The hollow carbon inner space can effectively encapsulate metallic Li through the porous inner wall and the lithophilic material. Additionally, the high modulus carbon shell serves as an interface layer to effectively inhibit Li dendrite growth and alleviate the volume effect during operation.

Cui's team applied a monolayer of amorphous hollow carbon nanospheres with an interconnected structure onto the surface of Li metal (Fig. 7a), effectively mitigating Li dendrites formation and facilitating the formation of stable SEI films<sup>[104]</sup>. The findings indicate that under  $1 \text{ mA cm}^{-2}$ , the formation of Li dendrites is not observed. The Coulombic efficiency was enhanced to 99% after 150 cycles. Compared to the unmodified sample, its electrochemical performance exhibited a significant improvement. Cui et al.

further investigated the Li nucleation mechanism on different metal substrate and discovered a substrate-dependent growth pattern, which manifests significant differences in Li nucleation barriers among different substrates. This finding enables selective Li deposition<sup>[105]</sup>. By utilizing binary phase diagrams, it has been determined that metals exhibiting a certain degree of solubility in Li do not have nucleation barriers. Therefore, a composite metal anode featuring a nanocapsular structure was developed by using hollow carbon spheres and nanoparticle seeds (Fig. 7b). During the plating process, Li primarily grew within the confines of these spheres. This selective growth and stable encapsulation effectively prevented Li dendrite formation.

The introduction of heterogeneous components in the recombination process of functionalized hollow carbon also possesses outstanding performance for constructing Li metal electrodes and inhibiting Li dendrites<sup>[106]</sup>. Wang et al. synthesized N-doped porous hollow carbon spheres by a simple and effective approach, which can serve as promising nano-encapsulation materials<sup>[107]</sup>. Each hollow porous carbon sphere is equipped with a lithophilic carbon shell featuring a dense N-rich layer on the inner shell layer, facilitating the selective Li plating into the carbon sphere (Fig. 7c). In situ electron microscopy has demonstrated that these N-doped porous hollow carbon spheres are capable of repeatedly and stably encapsulating Li metal. The  $\text{Li}^+$  can traverse multiple interconnected hollow carbon spheres to achieve uniform and long-range ordered deposition. Furthermore, Wang et al. have ingeniously designed carbon nanobowls (CBs) with outer surfaces featuring varying positive and negative curvatures (Fig. 7d), as well as fully enclosed inner cavities and semi-enclosed recessed spaces<sup>[108]</sup>. The growth behavior of Li metal under geometric guidance was further investigated *via in-situ* electron microscopy, using CBs as a model substrate. The results revealed that because of the surface curvature, Li metal preferentially plated on the concave of isolated CBs rather than on their convex surface. Fully confined cavities are more favorable for Li plating compared to partially confined spaces, such

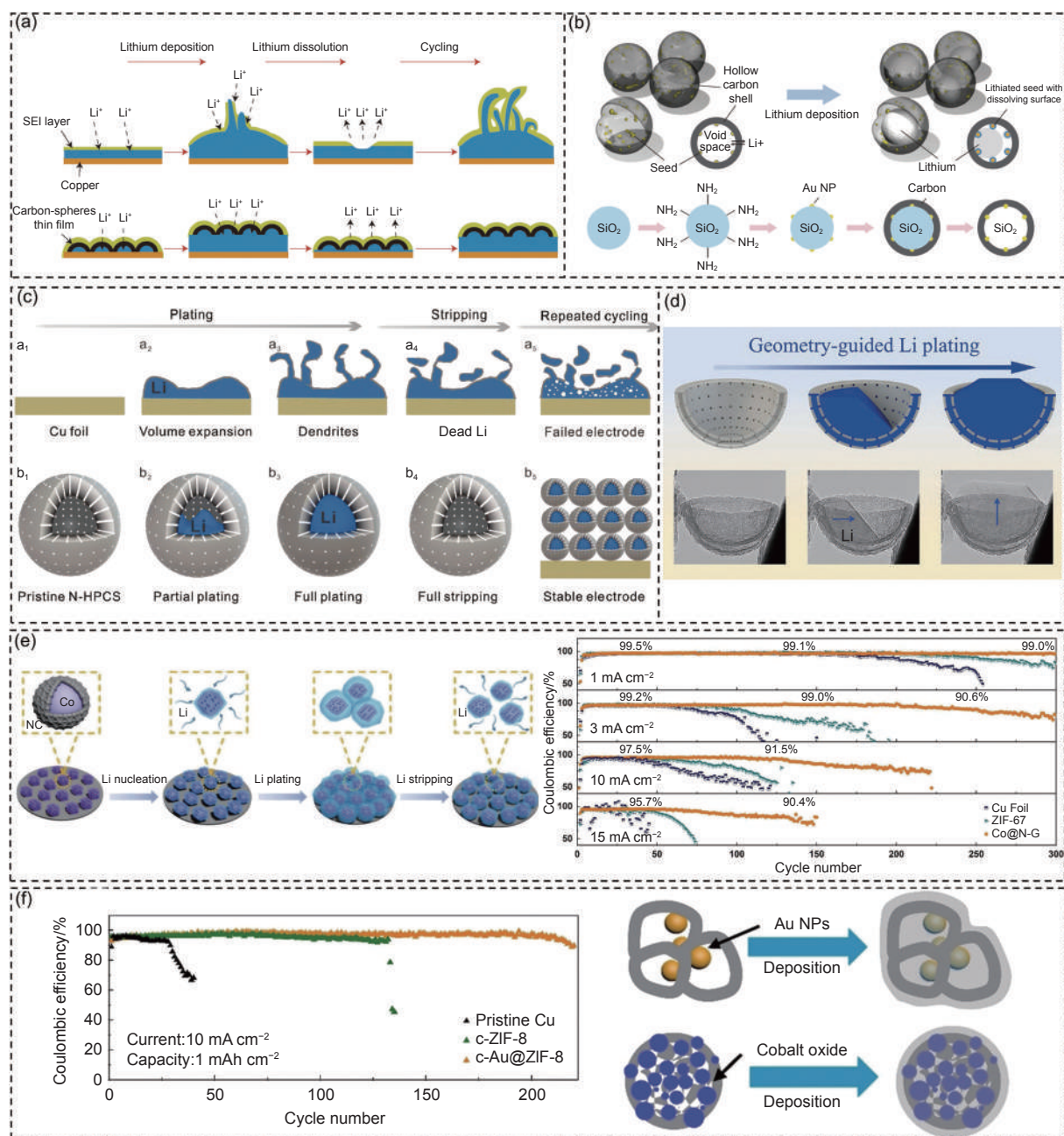


Fig. 7 (a) Schematic illustration of the Li plating/stripping behavior on different structures<sup>[104]</sup>. (b) Schematic illustration of Li metal nanocapsules design and preparation of hollow carbon with Au NPs<sup>[105]</sup>. (c) Schematic diagrams of the Li plating and stripping on Cu foil and N-HPCs<sup>[107]</sup>. (d) Schematic illustration and SEM images of Li plating on the CB<sup>[108]</sup>. (e) Schematic illustration of the Li nucleation and plating/stripping on the Co@N-G substrate. Coulombic efficiencies of different electrodes at 1, 3, 10, 15 mA cm<sup>-2</sup> with 1 mAh cm<sup>-2</sup><sup>[109]</sup>. (f) Schematic diagrams of the Li deposition on c-Au@ZIF-8 and TA-ZIF-67 host based electrodes. Coulombic efficiencies of different electrodes at 10 mA cm<sup>-2</sup> with 1 mAh cm<sup>-2</sup><sup>[111]</sup>. (Reprinted with permission)

as hemispherical concave cavities and gaps between adjacent hemispherical concave cavities.

Based on their periodic structure, metal-organic frameworks (MOFs) can serve as precursors for the preparation of hollow carbon materials. Fan et al. have successfully transformed ZIF-67 into a carbon material with cobalt active sites under rational control through one-step carbonization (Fig. 7e)<sup>[109]</sup>. The ho-

mogeneous dispersion of cobalt nanoparticles in nitrogen-doped porous graphene clusters through a one-step method demonstrated a synergistic enhancement of lithophilicity, resulting in a smooth and uniform process for Li nucleation and plating. In addition, the carbonized ZIF-67 exhibits optimized electrical conductivity and electrochemical active area that facilitates uniform electron dispersion and prevents charge

accumulation, thereby impeding Li dendrite growth and withstanding higher current densities. Additionally, this carbonized architecture provides ample internal and external space to accommodate Li plating/stripping without volumetric fluctuations. As anticipated, the electrode shows excellent cycling stability (130 cycles at  $10 \text{ mA cm}^{-2}$ , and 80 cycles at  $15 \text{ mA cm}^{-2}$ ). As is commonly known, MOF refers to a type of porous structural material that consists of metal ions and organic ligand clusters. Different types of metal ion MOFs serve different functions in the processing of carbon-based Li deposition substrates, including lithiophilic components such as  $\text{Zn}^{[110]}$ . Li et al. proposed a dual modulation strategy involving continuous Li nucleation and restricted growth by MOF-derived hollow capsules embedded with Au or Co-O nanoparticles with Li affinity as a non-homogeneous substrate (Fig. 7f)<sup>[111]</sup>. These nanoparticles can function as heterogeneous crystalline species with zero overpotential nucleation, facilitating the Li plating into the substrate cavity during the plating process. This results in the formation of a conformal Li coating on the interface of the substrate. Modulating the electrode structure with c-Au@ZIF-8 and TA-ZIF-67 effectively suppresses dendrite formation, enabling the cycling performance at  $10 \text{ mA cm}^{-2}$  for 220 cycles. The advanced structure's heterogeneous crystalline species and restricted domains synergistically prevent dendrite deposition, enhancing cycling stability and durability of LMBs anode.

Overall, unlike other carbon materials, hollow carbon allows for Li deposition within its internal cavity while the carbon shell acts as a SEI, effectively mitigating volume expansion and suppressing dendrite formation. However, the high SSA of the hollow carbon result in significant initial side reactions, exacerbating electrolyte consumption. Furthermore, the reasonable design of porous structure and distribution within hollow carbon walls is crucial in determining Li transport dynamics.

### 3.5 Other carbon materials

In addition to the abovementioned mainstream advanced carbon materials, a diverse range of other carbon materials such as graphite, graphene quantum dots, biochar and fullerene have been selected for

their ability to restrain the Li dendrites in electrolyte additives, SEI layers or deposition substrates.

Sun et al. employed a molecular tunnelling strategy to fabricate a superdense bulk diffusion Li conductor (BDLC) with abundant atomic channels (Fig. 8a)<sup>[112]</sup>. Pre-tunnelling through graphite layers (with a layer spacing of approximately 0.7 nm) established inter- and intra-layer channels for Li diffusion, introducing both vacant and lithiophilic sites. Unlike conventional surface diffusion/deposition mechanisms, atomic channels effectively mitigate dendritic problems caused by non-uniform surface deposition and enable rapid bulk diffusion. The *in-situ* visualization techniques also further confirmed the highly reversible and dendrite-free Li plating/stripping behavior in BDLC blocks. As a result, the symmetric cells can maintain stable operation with low polarization of 27 mV for more than 2 000 h. Yan et al. utilized hydrophobic graphite fluoride (GF) to react with molten Li metal at high temperatures, resulting in the formation of a SEI layer composed of GF and LiF on Li surface<sup>[113]</sup>. The SEI layer effectively shields the Li metal from water and oxygen in air, ensuring long-term stability (Fig. 8b). Additionally, the GF-LiF layer exhibits greater viscoelasticity than bare Li and is less susceptible to fracture, thereby inhibiting the Li dendrite growth and stabilizing the anode interface. Wang et al. constructed LiF-rich SEI by lithiating the anode of commercial surface-fluorinated mesocarbon microbeads (MCMB-F)<sup>[114]</sup>. This robust and LiF-riched SEI exhibits high interfacial energy, and effectively promotes the planar growth of Li (Fig. 8c). This results in large grain formation without dendrites and exhibits a smooth, dense structure. Simultaneously, it hinders the vertical infiltration into the LiF-enriched SEI to generate Li dendrites and restrains the proliferation of Li dendrites in the Li metal anode. At a discharge areal capacity of  $1.2 \text{ mAh cm}^{-2}$ , the anode can achieve a CE for Li plating/stripping exceeding 99.2% within 25 cycles. Qiao et al. demonstrated for the first time that a radio frequency sputtering of graphite/ $\text{SiO}_2$  ultra-thin bilayer on Li metal as a protective layer allows for uniform Li deposition<sup>[115]</sup>. The flexible graphite within the protective layer serves as an electronic bridge between the deposited Li and the Li foil,

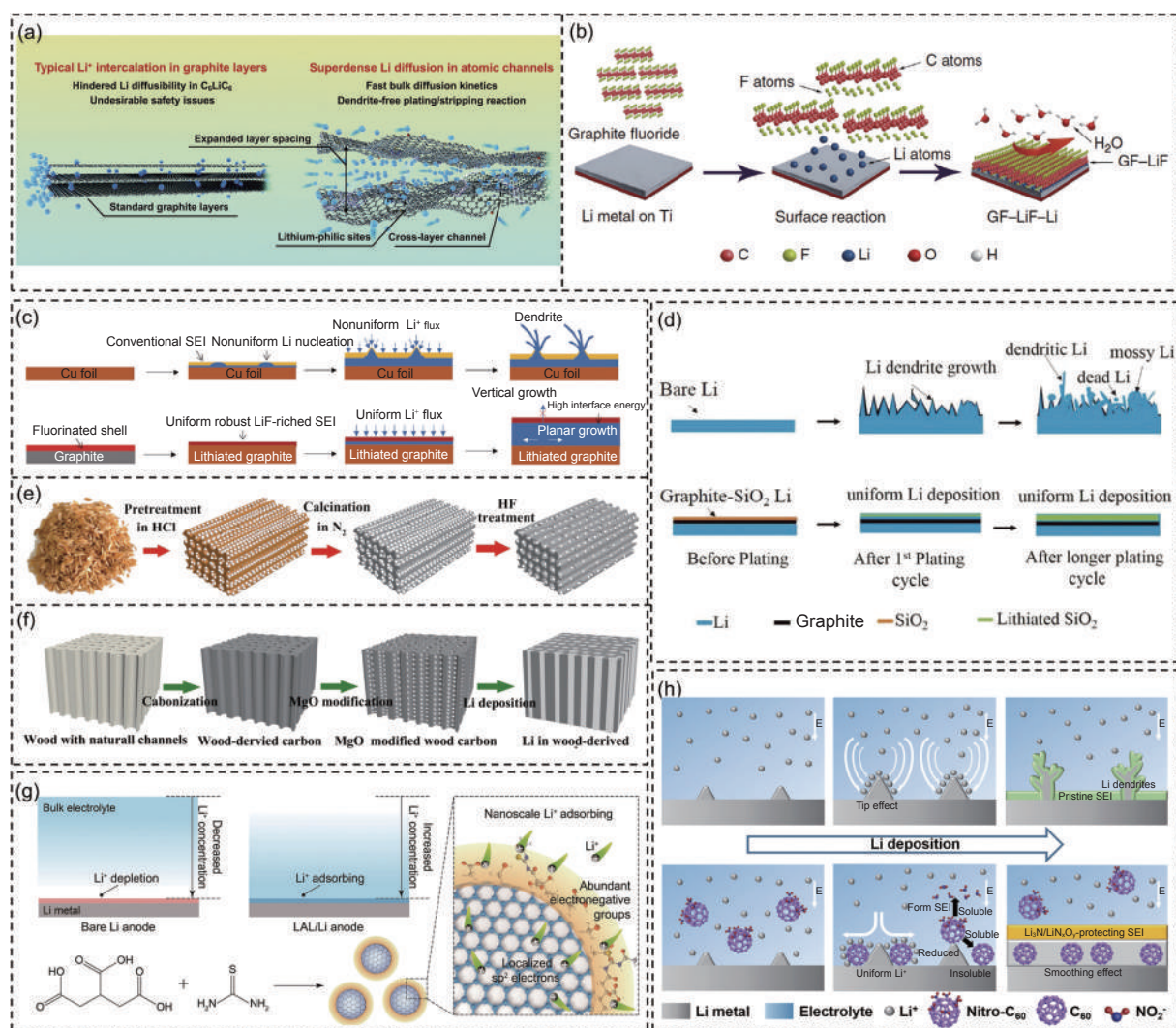


Fig. 8 (a) Schematic diagram of typical  $\text{Li}^+$  intercalation in graphite layers and superdense Li diffusion in atomic channels<sup>[112]</sup>. (b) Schematic diagram of the preparation and protective mechanism of GF-LiF-Li<sup>[113]</sup>. (c) Comparative schematic illustration of the Li deposition on Cu foil and MCMC-F electrode<sup>[114]</sup>. (d) Comparative schematic diagrams of the Li plating on Li with or without graphite-SiO<sub>2</sub> bilayer-modified<sup>[115]</sup>. (e) Schematic diagram of the preparation of RC<sup>[116]</sup>. (f) Schematic diagram of the preparation of MgO@WC/Li composite electrode<sup>[117]</sup>. (g) Comparative schematic diagrams of the  $\text{Li}^+$  in bare Li anode and LAL/Li anode upon Li deposition. And the preparation of the LAL<sup>[118]</sup>. (h) Schematic of the bifunctional effects of nitro-C60 additive<sup>[119]</sup>. (Reprinted with permission)

thereby reducing the dead Li and buffering volume effects resulting from Li deposition (Fig. 8d). The incorporation of SiO<sub>2</sub> enhances Li<sup>+</sup> conduction and redox reaction processes, provides high electrolyte infiltrability, electrochemical stability and mechanical modulus to inhibit the formation of Li dendrites.

Rice husk, due to its rich porous structure and high SiO<sub>2</sub> content, is widely utilized in the preparation of electrode materials such as silicon carbon and hard carbon. Building upon this foundation, Tao et al. have developed a multifunctional carbon (RC) extracted from rice husk to enhance Li anodes and S cathodes<sup>[116]</sup>. The RC was functionalized with F-contain-

ing groups on its surface, which facilitated the formation of high-efficiency SEI components and uniformly dispersed natural SiO<sub>2</sub> nanoparticles (Fig. 8e). These factors combined to create a porous structure that effectively controlled Li deposition, significantly reducing nucleation overpotential and improving coulombic efficiency. Tao et al. utilized balsa-derived porous carbon and metal oxide nanoparticles to construct Li deposition substrate, effectively reducing the barrier for lithium nucleation (Fig. 8f)<sup>[117]</sup>. The non-in situ observation follow the initial Li plating process confirms preferentially Li nucleation behavior in the step-edge region. This edge-guided effect may facilit-

ate Li stripping/plating primarily near the step region within the channel and inhibit negative dendrite formation. The modified Li anode exhibits the capability to operate at ultra-high current densities of  $15 \text{ mA cm}^{-2}$ , achieve a Coulombic efficiency of 96%, and demonstrate reduced nucleation barrier as well as improved cycling stability.

Peng et al. first proposed the ultrathin  $\text{Li}^+$  adsorption layer (LAL) composed of graphene quantum dots with polar functional groups on their surfaces (Fig. 8g)<sup>[118]</sup>. The high  $\text{Li}^+$  affinity of the quantum dots in LAL enables precise distribution of the  $\text{Li}^+$  flux at the solid-liquid interface, resulting in increased local  $\text{Li}^+$  flux and furtherly mitigating  $\text{Li}^+$  depletion under high rate. Simultaneously, the LAL allows for  $\text{Li}^+$  penetration, resulting in continuous  $\text{Li}^+$  adsorption effects and dendrite-free Li deposition. The efficiency Li deposition/dissolution exceeding 1 000 h can be achieved at high current densities ( $60 \text{ mA cm}^{-2}$ ) and areal capacities ( $60 \text{ mAh cm}^{-2}$ ), surpassing those of existing lithium anodes. Xie et al. utilized nitrofullerene  $\text{C}_{60}$  (nitro- $\text{C}_{60}$ ) as a bifunctional additive in electrolyte with a smoothing effect<sup>[119]</sup>. Nitro- $\text{C}_{60}$  can be attracted to anode protrusions through electrostatic adsorption and subsequently form  $\text{NO}_2^-$  and  $\text{C}_{60}$ . The uneven grooves on the surface of Li serve as anchoring sites for  $\text{C}_{60}$ , resulting in a flattened anode surface and more evenly distributed electric field, which ultimately leads to uniform  $\text{Li}^+$  distribution (Fig. 8h). Simultaneously, the  $\text{NO}_2^-$  anion and Li metal react to generate a robust SEI enriched with  $\text{Li}_3\text{N}$  and  $\text{LiN}_x\text{O}_y$  species, which facilitates efficient ion transport. Consequently, these modified Li anodes exhibit enhanced cycling life.

## 4 Conclusion and perspectives

LMBs, driven by high energy density demand, are the most promising candidates for next-generation high energy density energy storage systems. However, the unbridled Li deposition/stripping as well as the intense formation of dendrites continue to hinder the commercial application of LMBs. A more comprehensive explanation of the process behind Li dendrite formation is necessary in order to develop effective

prevention methods. In recent years, several models have been proposed to explain the formation of Li dendrites, including surface diffusion model, heterogeneous nucleation model, space charge model and SEI-induced nucleation model. These models contribute to a better knowledge of the mechanism behind Li dendrite formation. Although these models have certain prerequisites and limitations, they provide researchers with different perspectives to address the Li dendrite problem, such as electrolyte optimization, nucleation control, SEI modification, 3D substrate design, etc. Advanced carbon materials, such as graphene, CNTs, CFs and hollow carbons, are crucial in addressing the lithium dendrite issue on Li metal electrodes caused by their high electrical conductivity, chemical and electrochemical stability, excellent mechanical properties and plasticity.

Graphene and graphite exhibit superior film-forming properties compared to other carbon materials, making them ideal for constructing effective SEI layers that homogenize the distribution of interfacial electric fields and ion flux. Furthermore, through functionalization or combination with other lipophilic components, transport kinetics of  $\text{Li}^+$  are enhanced while nucleation barriers are reduced, effectively inhibiting the formation of Li dendrites. CNTs and CF, as one-dimensional materials in advanced carbon materials, possess inherent advantages over other carbon materials for constructing a 3D Li deposition substrate. In addition to their lightweight nature, the 3D substrate also exhibits high electrical conductivity and a large SSA. These properties effectively reduce local current density and transport kinetics, which are conducive to improving the critical formation conditions of Li dendrites according to Sand's law. Additionally, incorporating other lipophilic components into the 3D carbon substrate can further enhance the uniformity of Li deposition. Due to its lower commercial cost compared to CNTs, CF holds greater potential for application in Li metal electrodes. The structural advantages of hollow carbon enable it to deposit Li within its inner cavity and facilitate the construction of SEI through its carbon shell, which plays a crucial role in mitigating volume expansion and dendrite growth. However, its synthesis is complicated. In general, ad-

vanced carbon materials show great potential in inhibiting Li dendrite formation through a variety of tuning mechanisms, including, nucleation, diffusion, SEI control, and also by serving as deposition substrates, as shown in Table 1. However, there are still several issues and functional developments, as mentioned below, that require further understanding and development for the construction of high energy density LMBs using advanced carbon materials as composite electrodes:

(1) The carbon material's intrinsic properties, while advantageous for suppressing Li dendrites, also present some undesired issues. Its high SSA results in increased consumption of electrolyte and active Li sources during the initial electrochemical process for SEI construction. On the other hand, the high conductivity of carbon material as a 3D substrate facilitates rapid electron migration to different regions of the substrate, potentially resulting in preferential Li deposition near the electrolyte end and thus impeding dendrite suppression. Additionally, achieving a stable

SEI formation in the 3D carbon substrates during Li plating/stripping is challenging, and there remains controversy surrounding the existence and distribution of the SEI. Therefore, it is necessary to strike a better balance and further explore the constitutive relationship between structural design and performance optimization of carbon materials for Li metal electrode applications.

(2) The dendrite suppression mechanism of carbon materials is often attributed to the dispersion of the current density and homogenization of electric field, among other factors. However, this explanation is insufficient, particularly when considering composites of carbon materials with other substances. To optimize the structural design of carbon-based interfaces and 3D substrates, a more profound comprehension of the role of carbon materials in the Li plating/stripping process is necessary. Additionally, employing new characterization techniques to comprehend the function of carbon-based Li metal composite electrodes will aid in establishing principles of

**Table 1 Summary of the electrochemical performance of electrodes based on different advanced carbon materials**

Electrode	Symmetric cell	Full cell	Reference
SR-G-Li	1000 cycles at 5 mA cm <sup>-2</sup> , 1 mAh cm <sup>-2</sup>	LiFePO <sub>4</sub>   SR-G-Li, 1 C, 128.8 mAh g <sup>-1</sup> after 300 cycles	[72]
GBL	600 h at 3 mA cm <sup>-2</sup> , 3 mAh cm <sup>-2</sup>	LiFePO <sub>4</sub>   GBL  Li, 1C, 100 mAh g <sup>-1</sup> after 1600 cycles	[74]
NG basedLi metal anodes	150 cycles at 1 mA cm <sup>-2</sup> , 0.042 mAh cm <sup>-2</sup>	-	[77]
rGO-Cu <sub>2</sub> O/Cu@Li	300 h at 0.5 mA cm <sup>-2</sup>	LiFePO <sub>4</sub>   rGO-Cu <sub>2</sub> O/Cu@Li, 2 C, 94.3 mA h g <sup>-1</sup>	[80]
Layered Li-rGO electrodes	Beyond 100 cycles at 3 mA cm <sup>-2</sup> , mAh cm <sup>-2</sup>	LiCoO <sub>2</sub>   Li-rGO, 10 C, ~ 70 mAh g <sup>-1</sup>	[81]
Li-SiO <sub>2</sub> @ERG-CNF	1000 h at 0.5 mA cm <sup>-2</sup> , 1 mAh cm <sup>-2</sup>	LiFePO <sub>4</sub>   Li-SiO <sub>2</sub> @ERG-CNF, 1 C, 106.9 mAh g <sup>-1</sup> after 1000 cycles	[86]
Li@TLI-GO/Zn/CC	>1600 h at 1 mA cm <sup>-2</sup> , 1 mAh cm <sup>-2</sup>	LiFePO <sub>4</sub>   Li@TLI-GO/Zn/CC, 5 C, capacity retention of 94.6% after 3000 cycles	[7]
LiCSMF	2000 cycles at 40 mA cm <sup>-2</sup> , 2 mAh cm <sup>-2</sup>	S-CSMF  LiCSMF, 1 C, 200 cycles	[88]
GZCNT-coated Li	100 h at 10 mA cm <sup>-2</sup>	S  GZCNT-coated Li, 0.2 C, 1.73 mAh cm <sup>-2</sup> after 200 cycles	[91]
Li-CNT-AB	100 cycles at 3 mA cm <sup>-2</sup> , 1 mAh cm <sup>-2</sup>	LiFePO <sub>4</sub>   Li-CNT-AB, CE of ~ 98.7% after 700 cycles.	[93]
OPA-Li-CNT	200 cycles at 3 mA cm <sup>-2</sup> , 0.5 mAh cm <sup>-2</sup>	LiFePO <sub>4</sub>   OPA-Li-CNT, 1 C, 250 cycles	[94]
GCF@Li	over 300 h at 2 mA cm <sup>-2</sup>	LiFePO <sub>4</sub>   GCF@Li, 300 cycles with a capacity retention of 80%	[96]
CNF-TiN	200 cycles at 3 mA cm <sup>-2</sup>	LiFePO <sub>4</sub>   CNF-TiN, 122.4 mAh g <sup>-1</sup> after 250 cycles	[98]
Li/CF	90 h with a small polarization voltage of 120 mV	S  Li/CF, 3.25 mAh cm <sup>-2</sup> , 0.1 C, a capacity retention rate of 98% after 100 cycles	[99]
Li-C anode	500 h at 1 mA cm <sup>-2</sup> , 1 mAh cm <sup>-2</sup>	NMC  Li-C, 350-380 Wh kg <sup>-1</sup> for 200 cycles	[100]
Li@CF	270 cycles at 3 mA cm <sup>-2</sup> , 1 mAh cm <sup>-2</sup>	Mg/Ti-LiNiO <sub>2</sub>   Li@CF, 0.5 C, 127 mAh g <sup>-1</sup> after 140 cycles	[101]
CC-Zn-CMFs	2000 h at 1 mA cm <sup>-2</sup> , 1 mAh cm <sup>-2</sup>	Mg/Ti-LiNiO <sub>2</sub>   CC-Zn-CMFs-Li, 200 cycles without obvious capacity decay	[102]
SAFeNi@LNCP-Li	650 h at 5 mA cm <sup>-2</sup> , 20 mAh cm <sup>-2</sup>	SAFeNi@LNCP  SAFeNi@LNCP-Li, 5 C, 856 mA h g <sup>-1</sup>	[103]
N-HPCSs	-	N-HPCSs/S  Li/Cu@N-HPCSs, 1 C, 907 mAh g <sup>-1</sup> , a capacity retention rate of 80.1% after 400 cycles	[107]
Li-Co@N-G	1000 h at 1 mA cm <sup>-2</sup> , 1 mAh cm <sup>-2</sup>	NCM  Li-Co@N-G, 1 C, a capacity retention of 92% after 100 cycles	[109]
BDLC	2000 h at 1 mA cm <sup>-2</sup> , 1 mAh cm <sup>-2</sup>	100% capacity retention is achieved over 370 cycles	[112]
Li@MCMB-F	-	LiFePO <sub>4</sub>   Li@MCMB-F, 2.4 mAh cm <sup>-2</sup> for 110 times at a capacity decay of 0.01% per cycle	[114]
MgO@WC	-	LiCoO <sub>2</sub>   MgO@WC/Li, 1 C, 300 cycles	[117]
LAL/Li	>1000 h at 60 mA cm <sup>-2</sup> , 60 mAh cm <sup>-2</sup>	LAL/Li-air, stably cycled for over 450 cycles	[118]
Nitro-C <sub>60</sub>	>400 h at 1 mA cm <sup>-2</sup> , 1 mAh cm <sup>-2</sup>	S  Li, retention of 63.2% over 100 cycles	[119]

design in general.

(3) Currently, research on the application of Li metal electrodes supported by carbon materials has primarily been conducted using button cells and under ideal conditions for operation and testing. However, these conditions are insufficient for practical commercial applications. Therefore, it is crucial to evaluate the feasibility of carbon-based Li metal electrodes under realistic operating conditions. The key parameters governing the performance of carbon-based Li metal electrodes, as evaluated under test conditions such as pouch cell, are of paramount practical importance in guiding the design of carbon material interfaces, substrates and other functionalizations and structures. These parameters are crucial to promoting real-world applications of advanced carbon materials.

The application of LMBs still faces numerous challenges. The key to commercializing LMBs lies in solving the problem of Li dendrites on their electrodes. Advanced carbon materials, with delicate structure and chemical design advantages, exhibit great potential for addressing this issue. We believe that a more profound comprehension of the crucial parameters and mechanisms of carbon-based Li metal electrodes in practical applications will serve as a guide for further optimization and design of carbon material structures, thus expediting the development and application of LMBs.

## Acknowledgements

This work was supported by National Natural Science Foundation of China (22225801, 52072256) and Key R & D program of Shanxi Province (202102030201006, 202202070301016).

## References

- [ 1 ] Zhu Z, Jiang T, Ali M, et al. Rechargeable batteries for grid scale energy storage[J]. *Chemical Reviews*, 2022, 122(22): 16610-16751.
- [ 2 ] Shin C H, Lee H Y, Gyan-Barimah C, et al. Magnesium: Properties and rich chemistry for new material synthesis and energy applications[J]. *Chemical Society Reviews*, 2023, 52(6): 2145-2192.
- [ 3 ] Quilty C D, Wu D, Li W, et al. Electron and ion transport in lithium and lithium-ion battery negative and positive composite electrodes[J]. *Chemical Reviews*, 2023, 123(4): 1327-1363.
- [ 4 ] Kim S, Park G, Lee S J, et al. Lithium-metal batteries: From fundamental research to industrialization [J]. *Advanced Materials*, 2022: e2206625.
- [ 5 ] Piao Z, Gao R, Liu Y, et al. A Review on regulating Li<sup>+</sup> solvation structures in carbonate electrolytes for lithium metal batteries[J]. *Advanced Materials*, 2023, 35(15): e2206009.
- [ 6 ] Zhang H, Qiao L, Armand M. Organic electrolyte design for rechargeable batteries: From lithium to magnesium[J]. *Angewandte Chemie International Edition*, 2022, 61(52): e202214054.
- [ 7 ] Zhang N, Du L, Zhang J, et al. Self-assembled tent-like nanocavities for space-confined stable lithium metal anode[J]. *Advanced Functional Materials*, 2023, 33(16): 2210862.
- [ 8 ] Liu Y, Ju Z, Zhang B, et al. Visualizing the sensitive lithium with atomic precision: Cryogenic electron microscopy for batteries[J]. *Accounts of Chemical Research*, 2021, 54(9): 2088-2099.
- [ 9 ] Paul P P, Mcshane E J, Colclasure A M, et al. A review of existing and emerging methods for lithium detection and characterization in Li-ion and Li-metal batteries[J]. *Advanced Energy Materials*, 2021, 11(17): 2100372.
- [ 10 ] Zhang X, Yang Y, Zhou Z. Towards practical lithium-metal anodes[J]. *Chemical Society Reviews*, 2020, 49(10): 3040-3071.
- [ 11 ] Chen X R, Zhao B C, Yan C, et al. Review on Li deposition in working batteries: From nucleation to early growth[J]. *Advanced Materials*, 2021, 33(8): e2004128.
- [ 12 ] Wang Z, Sun Z, Li J, et al. Insights into the deposition chemistry of Li ions in nonaqueous electrolyte for stable Li anodes[J]. *Chemical Society Reviews*, 2021, 50(5): 3178-3210.
- [ 13 ] Santos E, Schmickler W. The crucial role of local excess charges in dendrite growth on lithium electrodes[J]. *Angewandte Chemie International Edition*, 2021, 60(11): 5876-5881.
- [ 14 ] Xiao J. How lithium dendrites form in liquid batteries[J]. *Science*, 2019, 366(6464): 426-427.
- [ 15 ] Zheng J, Kim M S, Tu Z, et al. Regulating electrodeposition morphology of lithium: towards commercially relevant secondary Li metal batteries[J]. *Chemical Society Reviews*, 2020, 49(9): 2701-2750.
- [ 16 ] Wei C, Zhang Y, Tian Y, et al. Design of safe, long-cycling and high-energy lithium metal anodes in all working conditions: Progress, challenges and perspectives[J]. *Energy Storage Materials*, 2021, 38: 157-89.
- [ 17 ] Li M, Wang C, Chen Z, et al. New concepts in electrolytes[J]. *Chemical Reviews*, 2020, 120(14): 6783-6819.
- [ 18 ] Kim K, Ma H, Park S, et al. Electrolyte-additive-driven interfacial engineering for high-capacity electrodes in lithium-ion batteries: Promise and challenges[J]. *ACS Energy Letters*, 2020, 5(5): 1537-1553.
- [ 19 ] Jie Y, Ren X, Cao R, et al. Advanced liquid electrolytes for rechargeable Li metal batteries[J]. *Advanced Functional Materials*, 2020, 30(25): 1910777.
- [ 20 ] Sheng O, Jin C, Ding X, et al. A decade of progress on solid-state electrolytes for secondary batteries: Advances and contributions[J]. *Advanced Functional Materials*, 2021, 31(27): 2100891.
- [ 21 ] Wu J, Li X, Rao Z, et al. Electrolyte with boron nitride nanosheets

- as leveling agent towards dendrite-free lithium metal anodes[J]. *Nano Energy*, 2020, 72: 104725.
- [22] Li S, Zhang W, Wu Q, et al. Synergistic dual-additive electrolyte enables practical lithium-metal batteries[J]. *Angew Chem Int Ed Engl*, 2020, 59(35): 14935-41.
- [23] Chen J, Fan X, Li Q, et al. Electrolyte design for LiF-rich solid-electrolyte interfaces to enable high-performance micro-sized alloy anodes for batteries[J]. *Nature Energy*, 2020, 5(5): 386-397.
- [24] Fan X, Ji X, Chen L, et al. All-temperature batteries enabled by fluorinated electrolytes with non-polar solvents[J]. *Nature Energy*, 2019, 4(10): 882-890.
- [25] Liu F, Wang L, Zhang Z, et al. A mixed lithium-ion conductive  $\text{Li}_2\text{S}/\text{Li}_2\text{Se}$  protection layer for stable lithium metal anode[J]. *Advanced Functional Materials*, 2020, 30(23): 2001607.
- [26] Yu Z, Cui Y, Bao Z. Design principles of artificial solid electrolyte interphases for lithium-metal anodes[J]. *Cell Reports Physical Science*, 2020, 1(7): 100119.
- [27] Yan C, Xu R, Xiao Y, et al. Toward critical electrode/electrolyte interfaces in rechargeable batteries[J]. *Advanced Functional Materials*, 2020, 30(23): 1909887.
- [28] Lu G, Nai J, Luan D, et al. Surface engineering toward stable lithium metal anodes[J]. *Science Advances*, 2023, 9(14): eadf1550.
- [29] Fang R, Han Z, Li J, et al. Rationalized design of hyperbranched trans-scale graphene arrays for enduring high-energy lithium metal batteries[J]. *Science Advances*, 2022, 8(34): eadc9961.
- [30] Zhao X, Xia S, Zhang X, et al. Highly lithiophilic copper-reinforced scaffold enables stable Li metal anode[J]. *ACS Applied Materials & Interfaces*, 2021, 13(17): 20240-20250.
- [31] Zou P, Chiang S W, Zhan H, et al. A Periodic "self-correction" scheme for synchronizing lithium plating/stripping at ultrahigh cycling capacity[J]. *Advanced Functional Materials*, 2020, 30(21): 1910532.
- [32] Yang T, Li L, Wu F, et al. A Soft lithiophilic graphene aerogel for stable lithium metal anode[J]. *Advanced Functional Materials*, 2020, 30(30): 2002013.
- [33] Brissot C, Rosso M, Chazalviel J N, et al. Dendritic growth mechanisms in lithium/polymer cells[J]. *Journal of power sources*, 1999, 81-82: 925-929.
- [34] Chen J, Zhao J, Lei L, et al. Dynamic intelligent Cu current collectors for ultrastable lithium metal anodes[J]. *Nano Letters*, 2020, 20(5): 3403-3410.
- [35] Zhang C, Lyu R, Lv W, et al. A lightweight 3D Cu nanowire network with phosphidation gradient as current collector for high-density nucleation and stable deposition of lithium[J]. *Advanced Materials*, 2019, 31(48): e1904991.
- [36] Jin C B, Shi P, Zhang X Q, et al. Advances in carbon materials for stable lithium metal batteries[J]. *New Carbon Materials*, 2022, 37(1): 1-24.
- [37] Yan X, Lin L, Chen Q, et al. Multifunctional roles of carbon-based hosts for Li-metal anodes: A review[J]. *Carbon Energy*, 2021, 3(2): 303-329.
- [38] Cheng Y, Chen J, Chen Y, et al. Lithium host: Advanced architecture components for lithium metal anode[J]. *Energy Storage Materials*, 2021, 38: 276-298.
- [39] Zhang L, Qin X, Zhao S, et al. Advanced matrixes for binder-free nanostructured electrodes in lithium-ion batteries[J]. *Advanced Materials*, 2020, 32(24): e1908445.
- [40] Myung S T, Hitoshi Y, Sun Y K. Electrochemical behavior and passivation of current collectors in lithium-ion batteries[J]. *Journal of Materials Chemistry*, 2011, 21(27): 9891-9911.
- [41] Shi P, Zhang X Q, Shen X, et al. A review of composite lithium metal anode for practical applications[J]. *Advanced Materials Technologies*, 2019, 5(1): 1900806.
- [42] Fang R, Chen K, Yin L, et al. The regulating role of carbon nanotubes and graphene in lithium-ion and lithium-sulfur batteries[J]. *Advanced Materials*, 2019, 31(9): e1800863.
- [43] Shen X, Zhang R, Shi P, et al. How does external pressure shape Li dendrites in Li metal batteries?[J]. *Advanced Energy Materials*, 2021, 11(10): 2003416.
- [44] Jana A, Woo S I, Vikrant K S N, et al. Electrochemomechanics of lithium dendrite growth[J]. *Energy & Environmental Science*, 2019, 12(12): 3595-3607.
- [45] Lin D, Liu Y, Pei A, et al. Nanoscale perspective: Materials designs and understandings in lithium metal anodes[J]. *Nano Research*, 2017, 10(12): 4003-4026.
- [46] Jäckle M, Helmbrecht K, Smits M, et al. Self-diffusion barriers: Possible descriptors for dendrite growth in batteries?[J]. *Energy & Environmental Science*, 2018, 11(12): 3400-3407.
- [47] Hao F, Verma A, Mukherjee P P. Electrodeposition stability of metal electrodes[J]. *Energy Storage Materials*, 2019, 20: 1-6.
- [48] Ling C, Banerjee D, Matsui M. Study of the electrochemical deposition of Mg in the atomic level: Why it prefers the non-dendritic morphology[J]. *Electrochimica Acta*, 2012, 76: 270-274.
- [49] Aurbach D, Gofer Y, Schechter A, et al. A comparison between the electrochemical behavior of reversible magnesium and lithium electrodes[J]. *Journal of Power Sources*, 2001, 97-98: 269-273.
- [50] Ely D R, García R E. Heterogeneous nucleation and growth of lithium electrodeposits on negative electrodes[J]. *Journal of The Electrochemical Society*, 2013, 160(4): A662-A668.
- [51] Chazalviel J. Electrochemical aspects of the generation of ramified metallic electrodeposits[J]. *Physical Review A*, 1990, 42(12): 7355-7367.
- [52] Fleury V V, Chazalviel J, Rosso M. Theory and experimental evidence of electroconvection around electrochemical deposits[J]. *Physical Review Letters*, 1992, 68(16): 2492-2495.
- [53] Jiang J, Pan Z, Kou Z, et al. Lithiophilic polymer interphase anchored on laser-punched 3D holey Cu matrix enables uniform lithium nucleation leading to super-stable lithium metal anodes[J]. *Energy Storage Materials*, 2020, 29: 84-91.
- [54] Zhang X, Wang S, Xue C, et al. Self-suppression of lithium dendrite in all-solid-state lithium metal batteries with poly(vinylidene difluoride)-based solid electrolytes[J]. *Advanced Materials*, 2019, 31(11): e1806082.
- [55] Cheng X B, Yan C, Chen X, et al. Implantable solid electrolyte interphase in lithium-metal batteries[J]. *Chem*, 2017, 2(2): 258-270.
- [56] Shen X, Zhang R, Chen X, et al. The failure of solid electrolyte interphase on Li metal anode: Structural uniformity or mechanical strength?[J]. *Advanced Energy Materials*, 2020, 10(10): 1903645.

- [ 57 ] Lu Y, Tu Z, Archer L A. Stable lithium electrodeposition in liquid and nanoporous solid electrolytes[J]. *Nature materials*, 2014, 13(10): 961-969.
- [ 58 ] Cao X, Ren X, Zou L, et al. Monolithic solid-electrolyte interphases formed in fluorinated orthoformate-based electrolytes minimize Li depletion and pulverization[J]. *Nature Energy*, 2019, 4(9): 796-805.
- [ 59 ] Amanchukwu C V, Yu Z, Kong X, et al. A new class of ionically conducting fluorinated ether electrolytes with high electrochemical stability[J]. *Journal of the American Chemical Society*, 2020, 142(16): 7393-7403.
- [ 60 ] Wan J, Xie J, Kong X, et al. Ultrathin, flexible, solid polymer composite electrolyte enabled with aligned nanoporous host for lithium batteries[J]. *Nature Nanotechnology*, 2019, 14(7): 705-711.
- [ 61 ] Pathak R, Chen K, Gurung A, et al. Fluorinated hybrid solid-electrolyte-interphase for dendrite-free lithium deposition[J]. *Nature Communications*, 2020, 11(1): 93.
- [ 62 ] Xu T, Gao P, Li P, et al. Fast-charging and ultrahigh-capacity lithium metal anode enabled by surface alloying[J]. *Advanced Energy Materials*, 2020, 10(8): 1902343.
- [ 63 ] Guo W, Han Q, Jiao J, et al. In situ Construction of robust biphasic surface layers on Li metal for Li-S batteries with long cycle life[J]. *Angewandte Chemie International Edition*, 2021, 133(13): 7343-7350.
- [ 64 ] Lin Y, Plaza-Rivera C O, Hu L, et al. Scalable dry-pressed electrodes based on holey graphene[J]. *Accounts of Chemical Research*, 2022, 55(20): 3020-3031.
- [ 65 ] Pan L, Luo Z, Zhang Y, et al. Seed-free selective deposition of lithium metal into tough graphene framework for stable lithium metal anode[J]. *ACS Applied Materials & Interfaces*, 2019, 11(47): 44383-44389.
- [ 66 ] Zhao B, Li B, Wang Z, et al. Uniform Li deposition sites provided by atomic layer deposition for the dendrite-free lithium metal anode[J]. *ACS Applied Materials & Interfaces*, 2020, 12(17): 19530-19538.
- [ 67 ] Dong L, Nie L, Liu W. Water-stable lithium metal anodes with ultrahigh-rate capability enabled by a hydrophobic graphene architecture[J]. *Advanced Materials*, 2020, 32(14): e1908494.
- [ 68 ] Liu L, Yin Y X, Li J Y, et al. Uniform lithium nucleation/growth induced by lightweight nitrogen-doped graphitic carbon foams for high-performance lithium metal anodes[J]. *Advanced Materials*, 2018, 30(10): 1706216.
- [ 69 ] Zhou Y, Zhang X, Ding Y, et al. Reversible deposition of lithium particles enabled by ultraconformal and stretchable graphene film for lithium metal batteries[J]. *Advanced Materials*, 2020, 32(48): e2005763.
- [ 70 ] Liu S, Xia X, Zhong Y, et al. 3D TiC/C core/shell nanowire skeleton for dendrite-free and long-life lithium metal anode[J]. *Advanced Energy Materials*, 2018, 8(8): 1702322.
- [ 71 ] Wang X, Huang R Q, Niu S Z, et al. Research progress on graphene-based materials for high-performance lithium-metal batteries[J]. *New Carbon Material*, 2021, 36(4): 711-728.
- [ 72 ] Bai M, Xie K, Yuan K, et al. A scalable approach to dendrite-free lithium anodes via spontaneous reduction of spray-coated graphene oxide layers[J]. *Advanced Materials*, 2018, 30(29): e1801213.
- [ 73 ] Gao Y, Yan Z, Gray J L, et al. Polymer-inorganic solid-electrolyte interphase for stable lithium metal batteries under lean electrolyte conditions[J]. *Nature Materials*, 2019, 18(4): 384-389.
- [ 74 ] Xu L, Zhang Q, Niu S, et al. Organic eutectic mixture incorporated with graphene oxide sheets as lithiophilic artificial protective layer for dendrite-free lithium metal batteries[J]. *Advanced Energy Materials*, 2023, 13(12): 2204214.
- [ 75 ] Zhang R, Cheng X B, Zhao C Z, et al. Conductive nanostructured scaffolds render low local current density to inhibit lithium dendrite growth[J]. *Advanced Materials*, 2016, 28(11): 2155-62.
- [ 76 ] Meng Q, Deng B, Zhang H, et al. Heterogeneous nucleation and growth of electrodeposited lithium metal on the basal plane of single-layer graphene[J]. *Energy Storage Materials*, 2019, 16: 419-425.
- [ 77 ] Zhang R, Chen X R, Chen X, et al. Lithiophilic sites in doped graphene guide uniform lithium nucleation for dendrite-free lithium metal anodes[J]. *Angewandte Chemie International Edition*, 2017, 56(27): 7764-7768.
- [ 78 ] Li Z, Li X, Zhou L, et al. A synergistic strategy for stable lithium metal anodes using 3D fluorine-doped graphene shuttle-implanted porous carbon networks[J]. *Nano Energy*, 2018, 49: 179-185.
- [ 79 ] Chen X, Chen X R, Hou T Z, et al. Lithiophilicity chemistry of heteroatom-doped carbon to guide uniform lithium nucleation in lithium metal anodes[J]. *Science Advances*, 2019, 5(2): eaau7728.
- [ 80 ] Chen M, Cheng L, Chen J, et al. Facile and scalable modification of a Cu current collector toward uniform Li deposition of the Li metal anode[J]. *ACS Applied Materials & Interfaces*, 2020, 12(3): 3681-3687.
- [ 81 ] Lin D, Liu Y, Liang Z, et al. Layered reduced graphene oxide with nanoscale interlayer gaps as a stable host for lithium metal anodes[J]. *Nature Nanotechnology*, 2016, 11(7): 626-632.
- [ 82 ] Wang H, Cao X, Gu H, et al. Improving lithium metal composite anodes with seeding and pillaring effects of silicon nanoparticles[J]. *ACS Nano*, 2020, 14(4): 4601-4608.
- [ 83 ] Fang Y, Zhang Y, Zhu K, et al. Lithiophilic three-dimensional porous  $Ti_3C_2T_x$ -rGO membrane as a stable scaffold for safe alkali metal (Li or Na) anodes[J]. *ACS Nano*, 2019, 13(12): 14319-14328.
- [ 84 ] Shi H, Zhang C J, Lu P, et al. Conducting and lithiophilic MXene/Graphene framework for high-capacity, dendrite-free lithium-metal anodes[J]. *ACS Nano*, 2019, 13(12): 14308-14318.
- [ 85 ] Ni S, Sheng J, Zhang C, et al. Dendrite-free lithium deposition and stripping regulated by aligned microchannels for stable lithium metal batteries[J]. *Advanced Functional Materials*, 2022, 32(21): 2200682.
- [ 86 ] Song Q, Yan H, Liu K, et al. Vertically grown edge-rich graphene nanosheets for spatial control of Li nucleation[J]. *Advanced Energy Materials*, 2018, 8(22): 1800564.
- [ 87 ] Zhai P, Wang T, Jiang H, et al. 3D artificial solid-electrolyte interphase for lithium metal anodes enabled by insulator-metal-insulator layered heterostructures[J]. *Advanced Materials*, 2021, 33(13): e2006247.
- [ 88 ] Wang Z Y, Lu Z X, Guo W, et al. A dendrite-free lithium/carbon nanotube hybrid for lithium-metal batteries[J]. *Advanced*

- Materials, 2021, 33(4): e2006702.
- [ 89 ] Sun Z, Jin S, Jin H, et al. Robust expandable carbon nanotube scaffold for ultrahigh-capacity lithium-metal anodes[J]. *Advanced Materials*, 2018, 30(32): e1800884.
- [ 90 ] Liu F, Xu R, Hu Z, et al. Regulating lithium nucleation via CNTs modifying carbon cloth film for stable Li metal anode[J]. *Small*, 2019, 15(5): e1803734.
- [ 91 ] Zhang H, Liao X, Guan Y, et al. Lithiophilic-lithiophobic gradient interfacial layer for a highly stable lithium metal anode[J]. *Nature Communications*, 2018, 9(1): 3729.
- [ 92 ] Wang X, Pan Z, Yang J, et al. Stretchable fiber-shaped lithium metal anode[J]. *Energy Storage Materials*, 2019, 22: 179-184.
- [ 93 ] Guo F, Wang Y, Kang T, et al. A Li-dual carbon composite as stable anode material for Li batteries[J]. *Energy Storage Materials*, 2018, 15: 116-123.
- [ 94 ] Kang T, Wang Y, Guo F, et al. Self-assembled monolayer enables slurry-coating of Li Anode[J]. *ACS Central Science*, 2019, 5(3): 468-476.
- [ 95 ] Zhan Y X, Shi P, Jin C B, et al. Regulating the two-stage accumulation mechanism of inactive lithium for practical composite lithium metal anodes[J]. *Advanced Functional Materials*, 2022, 32(43): 2206834.
- [ 96 ] Zuo T T, Wu X W, Yang C P, et al. Graphitized carbon fibers as multifunctional 3D current collectors for high areal capacity Li anodes[J]. *Advanced Materials*, 2017, 29(29): 1700389.
- [ 97 ] Chen Y, Elangovan A, Zeng D, et al. Vertically aligned carbon nanofibers on Cu foil as a 3D current collector for reversible Li plating/stripping toward high-performance Li-S batteries[J]. *Advanced Functional Materials*, 2019, 30(4): 1906444.
- [ 98 ] Lin K, Qin X, Liu M, et al. Ultrafine titanium nitride sheath decorated carbon nanofiber network enabling stable lithium metal anodes[J]. *Advanced Functional Materials*, 2019, 29(46): 1903229.
- [ 99 ] Shi P, Li T, Zhang R, et al. Lithiophilic LiC(6) layers on carbon hosts enabling stable Li metal anode in working batteries[J]. *Advanced Materials*, 2019, 31(8): e1807131.
- [ 100 ] Niu C, Pan H, Xu W, et al. Self-smoothing anode for achieving high-energy lithium metal batteries under realistic conditions[J]. *Nature Nanotechnology*, 2019, 14(6): 594-601.
- [ 101 ] Tao L, Hu A, Yang Z, et al. A surface chemistry approach to tailoring the hydrophilicity and lithiophilicity of carbon films for hosting high-performance lithium metal anodes[J]. *Advanced Functional Materials*, 2020, 30(31): 2000585.
- [ 102 ] Fang Y, Zeng Y, Jin Q, et al. Nitrogen-doped amorphous Zn-carbon multichannel fibers for stable lithium metal anodes[J]. *Angewandte Chemie International Edition*, 2021, 60(15): 8515-8520.
- [ 103 ] Wang J, Zhang J, Duan S, et al. Lithium atom surface diffusion and delocalized deposition propelled by atomic metal catalyst toward ultrahigh-capacity dendrite-free lithium anode[J]. *Nano Letters*, 2022, 22(19): 8008-8017.
- [ 104 ] Zheng G, Lee S W, Liang Z, et al. Interconnected hollow carbon nanospheres for stable lithium metal anodes[J]. *Nature Nanotechnology*, 2014, 9(8): 618-623.
- [ 105 ] Yan K, Lu Z, Lee H W, et al. Selective deposition and stable encapsulation of lithium through heterogeneous seeded growth[J]. *Nature Energy*, 2016, 1(3): 16010.
- [ 106 ] Zhang T, Lu H, Yang J, et al. Stable lithium metal anode enabled by a lithiophilic and electron/ion conductive framework[J]. *ACS Nano*, 2020, 14(5): 5618-5627.
- [ 107 ] Ye W, Pei F, Lan X, et al. Stable nano-encapsulation of lithium through seed-free selective deposition for high-performance Li battery anodes[J]. *Advanced Energy Materials*, 2020, 10(7): 1902956.
- [ 108 ] Ye W, Wang L, Yin Y, et al. Lithium storage in bowl-like carbon: The effect of surface curvature and space geometry on Li metal deposition[J]. *ACS Energy Letters*, 2021, 6(6): 2145-2152.
- [ 109 ] Wang T S, Liu X, Zhao X, et al. Regulating uniform Li plating/stripping via dual-conductive metal-organic frameworks for high-rate lithium metal batteries[J]. *Advanced Functional Materials*, 2020, 30(16): 2000786.
- [ 110 ] Kim J, Lee J, Yun J, et al. Functionality of dual-phase lithium storage in a porous carbon host for lithium-metal anode[J]. *Advanced Functional Materials*, 2020, 30(15): 1910538.
- [ 111 ] Huang M, Yao Z, Yang Q, et al. Consecutive nucleation and confinement modulation towards Li plating in seeded capsules for durable Li-metal batteries[J]. *Angewandte Chemie International Edition*, 2021, 60(25): 14040-14050.
- [ 112 ] Zhou S, Chen W, Shi J, et al. Efficient diffusion of superdense lithium via atomic channels for dendrite-free lithium-metal batteries[J]. *Energy & Environmental Science*, 2022, 15(1): 196-205.
- [ 113 ] Shen X, Li Y, Qian T, et al. Lithium anode stable in air for low-cost fabrication of a dendrite-free lithium battery[J]. *Nature Communications*, 2019, 10(1): 900.
- [ 114 ] Cui C, Yang C, Eidson N, et al. A highly reversible, dendrite-free lithium metal anode enabled by a lithium-fluoride-enriched interphase[J]. *Advanced Materials*, 2020, 32(12): e1906427.
- [ 115 ] Pathak R, Chen K, Gurung A, et al. Ultrathin bilayer of graphite/SiO<sub>2</sub> as solid interface for reviving Li metal anode[J]. *Advanced Energy Materials*, 2019, 9(36): 1901486.
- [ 116 ] Jin C, Sheng O, Zhang W, et al. Sustainable, inexpensive, naturally multi-functionalized biomass carbon for both Li metal anode and sulfur cathode[J]. *Energy Storage Materials*, 2018, 15: 218-225.
- [ 117 ] Jin C, Sheng O, Lu Y, et al. Metal oxide nanoparticles induced step-edge nucleation of stable Li metal anode working under an ultrahigh current density of 15 mA cm<sup>-2</sup>[J]. *Nano Energy*, 2018, 45: 203-209.
- [ 118 ] Ye L, Liao M, Cheng X, et al. Lithium-metal anodes Working at 60 mA cm<sup>-2</sup> and 60 mAh cm<sup>-2</sup> through nanoscale lithium-ion adsorbing[J]. *Angewandte Chemie International Edition*, 2021, 60(32): 17419-17425.
- [ 119 ] Jiang Z, Zeng Z, Yang C, et al. Nitrofullerene, a C<sub>60</sub>-based bifunctional additive with smoothing and protecting effects for stable lithium metal anode[J]. *Nano Letters*, 2019, 19(12): 8780-8786.

